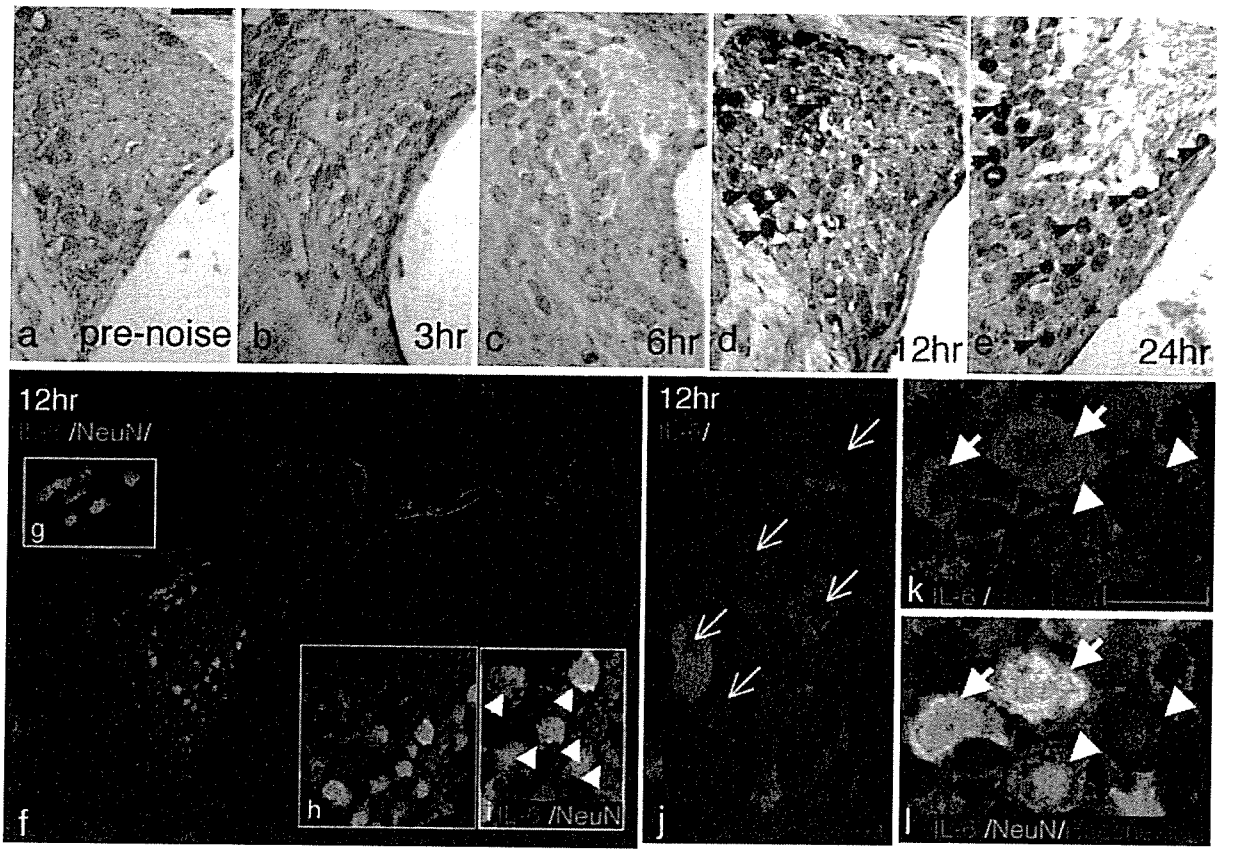

Fig. 6. Time-dependent expression of IL-6 in spiral ganglion after noise overstimulation. In the spiral ganglion, IL-6 immunoreactivity was also observed after noise exposure. The stainings were determined in the spiral ganglion of upper-basal turn of cochleae. The number of IL-6 immunolabeled ganglion cells increased markedly at 12 and 24 hr after noise exposure (**d,e**). **f–i:** Double-immunolabeling for IL-6 (red) and NeuN (green: a mature neuron marker). Higher power photos show IL-6 immunoreactivties on the surface of ganglion cells (h,i,**k,l**; arrowheads) and in the cytoplasm of some ganglion neurons (**j–l**; arrow). **a:** Control cochlea; **b–e:** 3, 6, 12, 24 hr after noise exposure; f–l: 12 hr after noise exposure. Red, IL-6; green, NeuN; blue, Hoechst. k,l: confocal images. Scale bars = a–e, 50 μm; f–l, 20 μm.

geting a specific proinflammatory cytokine, like IL-6, against noise-induced hearing loss.

ACKNOWLEDGMENTS

We are grateful to Dr. K. Dan for detailed instructions and suggestions regarding the RT-PCR and real-time RT-PCR experiments. We are grateful to all of the Okano laboratory's staff, especially to Dr. S. Shibata for critical suggestions regarding immunohistochemistry studies, and to our ENT department colleagues for valuable open discussions. This work was supported by Keio University Grant-in-Aid for Encouragement of Young Medical Scientists, grants from the Japan Science and Technology Agency, Core Research for Evolutional Science and Technology, a Grant-in-Aid for the 21st Century Center of Excellence (COE) program to Keio University from the Japanese Ministry of Education, Culture, Sports, Science and Technology (MEXT), and Grant-in-Aid for Young Scientists (B) to M.F. from the MEXT.

REFERENCES

Acarin L, Gonzalez B, Castellano B. 2000. Neuronal, astroglial and microglial cytokine expression after an excitotoxic lesion in the immature rat brain. Eur J Neurosci 12:3505–3520.

Allan SM, Rothwell NJ. 2001. Cytokines and acute neurodegeneration. Nat Rev Neurosci 2:734–744.

Berti R, Williams AJ, Moffett JR, Hale SL, Velarde LC, Elliott PJ, Yao C, Dave JR, Tortella FC. 2002. Quantitative real-time RT-PCR analysis of inflammatory gene expression associated with ischemia-reperfusion brain injury. J Cereb Blood Flow Metab 22:1068–1079.

Block F, Peters M, Nolden-Koch M. 2000. Expression of IL-6 in the ischemic penumbra. Neuroreport 11:963–967.

Buckley CD, Pilling D, Lord JM, Akbar AN, Scheel-Toellner D, Salmon M. 2001. Fibroblasts regulate the switch from acute resolving to chronic persistent inflammation. Trends Immunol 22:199–204.

Crouch JJ, Sakaguchi N, Lytle C, Schulte BA. 1997. Immunohistochemical localization of the Na-K-Cl co-transporter (NKCC1) in the gerbil inner ear. J Histochem Cytochem 45:773–778.

Flagella M, Clarke LL, Miller ML, Erway LC, Giannella RA, Andringa A, Gawenis LR, Kramer J, Duffy JJ, Doetschman T, Lorenz JN, Yamoah EN, Cardell EL, Shull GE. 1999. Mice lacking the basolateral

Na-K-2Cl cotransporter have impaired epithelial chloride secretion and are profoundly deaf. J Biol Chem 274:26946–26955.

Hashimoto S, Billings P, Harris JP, Firestein GS, Keithley EM. 2005. Innate immunity contributes to cochlear adaptive immune responses. Audiol Neurootol 10:35–43.

Hirose K, Discolo CM, Keasler JR, Ransohoff R. 2005. Mononuclear phagocytes migrate into the murine cochlea after acoustic trauma. J Comp Neurol 489:180–194.

Hirose K, Liberman MC. 2003. Lateral wall histopathology and endocochlear potential in the noise-damaged mouse cochlea. J Assoc Res Otolaryngol 4:339–352.

Hoya N, Okamoto Y, Kamiya K, Fujii M, Matsunaga T. 2004. A novel animal model of acute cochlear mitochondrial dysfunction. Neuroreport 15:1597–1600.

Ichimiya I, Yoshida K, Hirano T, Suzuki M, Mogi G. 2000. Significance of spiral ligament fibrocytes with cochlear inflammation. Int J Pediatr Otorhinolaryngol 56:45–51.

Ichimiya I, Yoshida K, Suzuki M, Mogi G. 2003. Expression of adhesion molecules by cultured spiral ligament fibrocytes stimulated with proinflammatory cytokines. Ann Otol Rhinol Laryngol 112:722–728.

Ito H, Takazoe M, Fukuda Y, Hibi T, Kusugami K, Andoh A, Matsumoto T, Yamamura T, Azuma J, Nishimoto N, Yoshizaki K, Shimoyama T, Kishimoto T. 2004. A pilot randomized trial of a human anti-interleukin-6 receptor monoclonal antibody in active Crohn's disease. Gastroenterology 126:989–996; discussion 947.

Karlidag T, Yalcin S, Ozturk A, Ustundag B, Gok U, Kaygusuz I, Susaman N. 2002. The role of free oxygen radicals in noise induced hearing loss: effects of melatonin and methylprednisolone. Auris Nasus Larynx 29:147–152.

Kikuchi T, Kimura RS, Paul DL, Takasaka T, Adams JC. 2000. Gap junction systems in the mammalian cochlea. Brain Res Brain Res Rev 32:163–166.

Komeda M, Roessler BJ, Raphael Y. 1999. The influence of interleukin-1 receptor antagonist transgene on spiral ganglion neurons. Hear Res 131:1–10.

Lim DJ. 1976. Ultrastructural cochlear changes following acoustic hyperstimulation and ototoxicity. Ann Otol Rhinol Laryngol 85:740–751.

Lin MT, Juan CY, Chang KJ, Chen WJ, Kuo ML. 2001. IL-6 inhibits apoptosis and retains oxidative DNA lesions in human gastric cancer AGS cells through upregulation of anti-apoptotic gene mcl-1. Carcinogenesis 22:1947–1953.

Lo EH, Dalkara T, Moskowitz MA. 2003. Mechanisms, challenges and opportunities in stroke. Nat Rev Neurosci 4:399–415.

Maeda K, Yoshida K, Ichimiya I, Suzuki M. 2005. Dexamethasone inhibits tumor necrosis factor-alpha-induced cytokine secretion from spiral ligament fibrocytes. Hear Res 202:154–160.

Mor A, Abramson SB, Pillinger MH. 2005. The fibroblast-like synovial cell in rheumatoid arthritis: a key player in inflammation and joint destruction. Clin Immunol 115:118–128.

Morganti-Kossmann MC, Rancan M, Stahel PF, Kossmann T. 2002. Inflammatory response in acute traumatic brain injury: a double-edged sword. Curr Opin Crit Care 8:101–105.

Murata J, Murayama A, Horii A, Doi K, Harada T, Okano H, Kubo T. 2004. Expression of Musashi1, a neural RNA-binding protein, in the cochlea of young adult mice. Neurosci Lett 354:201–204.

Nishimoto N, Kanakura Y, Aozasa K, Johkoh T, Nakamura M, Nakano S, Nakano N, Ikeda Y, Sasaki T, Nishioka K, Hara M, Taguchi H, Kimura Y, Kato Y, Asaoku H, Kumagai S, Kodama F, Nakahara H, Hagihara K, Yoshizaki K, Kishimoto T. 2005. Humanized anti-interleukin-6 receptor antibody treatment of multicentric Castleman's disease. Blood 106:2627–2632.

Nishimoto N, Yoshizaki K, Miyasaka N, Yamamoto K, Kawai S, Takeuchi T, Hashimoto J, Azuma J, Kishimoto T. 2004. Treatment of rheumatoid arthritis with humanized anti-interleukin-6 receptor antibody: a multicenter, double-blind, placebo-controlled trial. Arthritis Rheum 50:1761–1769.

Okada S, Nakamura M, Mikami Y, Shimazaki T, Mihara M, Ohsugi Y, Iwamoto Y, Yoshizaki K, Kishimoto T, Toyama Y, Okano H. 2004. Blockade of interleukin-6 receptor suppresses reactive astrogliosis and ameliorates functional recovery in experimental spinal cord injury. J Neurosci Res 76:265–276.

Pier GB, Lyczak JB, Wetzeler LM. 2004. Immunology, infection, and immunity. In: Pier GB, editor. Herndon, VA: American Society for Microbiology.

Satoh H, Firestein GS, Billings PB, Harris JP, Keithley EM. 2002. Tumor necrosis factor-alpha, an initiator, and etanercept, an inhibitor of cochlear inflammation. Laryngoscope 112:1627–1634.

Satoh H, Firestein GS, Billings PB, Harris JP, Keithley EM. 2003. Proinflammatory cytokine expression in the endolymphatic sac during inner ear inflammation. J Assoc Res Otolaryngol 4:139–147.

Shizuki K, Ogawa K, Matsunobu T, Kanzaki J, Ogita K. 2002. Expression of c-Fos after noise-induced temporary threshold shift in the guinea pig cochlea. Neurosci Lett 320:73–76.

Spicer SS, Schulte BA. 1991. Differentiation of inner ear fibrocytes according to their ion transport related activity. Hear Res 56:53–64.

Spicer SS, Schulte BA. 1996. The fine structure of spiral ligament cells relates to ion return to the stria and varies with place-frequency. Hear Res 100:80–100.

Suzuki S, Tanaka K, Nogawa S, Nagata E, Ito D, Dembo T, Fukuuchi Y. 1999. Temporal profile and cellular localization of interleukin-6 protein after focal cerebral ischemia in rats. J Cereb Blood Flow Metab 19:1256–1262.

Takemura K, Komeda M, Yagi M, Himeno C, Izumikawa M, Doi T, Kuriyama H, Miller JM, Yamashita T. 2004. Direct inner ear infusion of dexamethasone attenuates noise-induced trauma in guinea pig. Hear Res 196:58–68.

Wang X, Truong T, Billings PB, Harris JP, Keithley EM. 2003. Blockage of immune-mediated inner ear damage by etanercept. Otol Neurotol 24:52–57.

Webster M, Webster DB. 1981. Spiral ganglion neuron loss following organ of Corti loss: a quantitative study. Brain Res 212:17–30.

Yamashita D, Jiang HY, Schacht J, Miller JM. 2004. Delayed production of free radicals following noise exposure. Brain Res 1019:201–209.

Yamashita T, Sawamoto K, Suzuki S, Suzuki N, Adachi K, Kawase T, Mihara M, Ohsugi Y, Abe K, Okano H. 2005. Blockade of interleukin-6 signaling aggravates ischemic cerebral damage in mice: possible involvement of Stat3 activation in the protection of neurons. J Neurochem 94:459–468.

Yokota S, Miyamae T, Imagawa T, Iwata N, Katakura S, Mori M, Woo P, Nishimoto N, Yoshizaki K, Kishimoto T. 2005. Therapeutic efficacy of humanized recombinant anti-interleukin-6 receptor antibody in children with systemic-onset juvenile idiopathic arthritis. Arthritis Rheum 52:818–825.

Yoshida K, Ichimiya I, Suzuki M, Mogi G. 1999. Effect of proinflammatory cytokines on cultured spiral ligament fibrocytes. Hear Res 137:155–159.

Original Paper

Audiology & Neurotology

Audiol Neurotol 2007;12:119–126
DOI: 10.1159/000097798

Received: September 19, 2005
Accepted after revision: September 15, 2006
Published online: December 6, 2006

Sendai Virus Vector-Mediated Transgene Expression in the Cochlea in vivo

Sho Kanzaki[a] Akihiro Shiotani[a, b] Makoto Inoue[c] Mamoru Hasegawa[c] Kaoru Ogawa[a]

[a]Department of Otolaryngology, Keio University, Tokyo, [b]Department of Otolaryngology, National Defense Medical College, Tokorozawa, and [c]DNAVEC Corporation, Tsukuba, Japan

Key Words
Sendai virus vector · Gene transfer · Scala tympani · Scala media · Cochlea · Guinea pig

Abstract
We injected a recombinant Sendai virus (SeV) vector into the guinea pig cochlea using two different approaches – the scala media and scala tympani – and investigated which cell types took up the vector. The hearing threshold shift and distribution of transfected cells in animals using the scala media approach were different compared to those using the scala tympani approach. SeV can transfect very different types of cells, including stria vascularis, spiral ganglion neurons, and sensory epithelia of the organ of Corti, and fibrocytes of the scala tympani. Because SeV vectors can potentially deliver stimuli to the cochlea to induce hair cell regeneration, it may be a powerful tool for repairing the organ of Corti.

Introduction

Gene transfer into inner ear organs is an attractive new approach for treating hearing disorders. This technology can also be useful for treating sensorineural hearing loss, such as inherited deafness [Kanzaki et al., 2002a]. Various viral vectors are capable of carrying out gene transfer. Adenoviruses (AVs) are the most commonly used vectors in experimental studies involving hearing disorders [Kanzaki et al., 2002b, c]. In guinea pigs, adeno-associated virus vectors [Di Pasquale et al., 2005; Lalwani et al., 1996] and herpes simplex virus vectors [Geschwind et al., 1996] have been successfully used for gene transfer into the inner ear. In addition, a new generation of AV vectors has been shown to successfully transfect a few sensory epithelial cells in the guinea pig cochlea [Luebke et al., 2001].

Vectors can be injected into the cochlea through two approaches – the scala media and scala tympani. Of the two, the scala tympani approach minimizes cochlear damage, and thus has been preferred for many gene transfer studies [Kanzaki et al., 2002c; Kawamoto et al., 2004; Yagi et al., 1999]. The scala tympani approach is particularly useful when targeting spiral ganglion neurons, because vectors are taken up selectively by scala tympani fibrocytes, which in turn act as carriers for the delivery to the spiral ganglion neurons. AV-glial cell line-derived neurotrophic factor injections into the scala tympani spare hair cells [Yagi et al., 1999] and spiral ganglion cells [Kanzaki et al., 2002c; Yagi et al., 2000], while effectively delivering glial cell line-derived neurotrophic factor to spiral ganglion neurons. On the other hand, the scala media approach is useful when targeting hair cells for regeneration [Kawamoto et al., 2003]. AV vector injections into the scala media result in reporter transgene expression in supporting cells [Ishimoto et al., 2002], indicating that this vector successfully reaches the sensory epithelial cells.

KARGER
Fax +41 61 306 12 34
E-Mail karger@karger.ch
www.karger.com

1420–3030/07/0122–0119$23.50/0

Accessible online at:
www.karger.com/aud

Sho Kanzaki, MD, PhD
35 Shinanomachi, Shinjuku
Tokyo 160-0016 (Japan)
Tel. +81 3 3353 1211, Fax +81 3 3353 1261
E-Mail skan@sc.itc.keio.ac.jp

Injection via the scala media with AV containing *Atoh1*, a mouse homolog of the *Drosophila* gene *atonal*, caused hair cell regeneration by inducing transdifferentiation of supporting cells [Izumikawa et al., 2005]. The drawback with scala media injections is that such injections may produce an excessive volume of the vector in endolymph or may result in mechanical contact.

Although AVs are effective in transferring genes in clinical situations [Verma and Weitzman, 2005], one problem is that the host response to gene therapy vector exposure involves both the innate and adaptive immune systems. The initial innate immune response also plays a significant role in acute toxicity owing to AV vector exposure [Nazir and Metcalf, 2005]. The cytopathic and immunogenic nature of AV, therefore, precludes its use as transgene vectors for treating hearing disorders in humans. Thus, to make this new technology feasible in humans, it is necessary to develop novel viral vectors that are efficiently transported within the middle and inner ear, but do not produce significant cytopathic and immunogenic responses.

One promising viral vector is Sendai virus (SeV), a member of the Paramyxoviridae family. SeV is an enveloped virus that has nonsegmented, negative-sense genomic RNA [Sakai et al., 1999]. Its replication and gene expression is driven by viral RNA polymerase strictly through a cytoplasmic mechanism [Nakanishi et al., 1998]. SeV vectors have been shown to deliver transgenes to respiratory [Inoue et al., 2004; Yonemitsu et al., 2000], vascular [Masaki et al., 2001], and muscle systems [Shiotani et al., 2001] and neurons [Shirakura et al., 2004]. Now SeV is tested in clinical trials for arteriosclerosis of the lower limbs in Japan.

There are three advantages to using SeV vectors for human gene therapy. First, SeV vectors are completely free of genotoxicity [Bitzer et al., 2003; Griesenbach et al., 2005]. SeV vectors replicate and transcribe transgenes only in the cytoplasm, importantly avoiding interaction with host chromosomes. Second, SeV vectors have remarkably high transfection efficiency in many tissues and cell types. Gene transfer to the respiratory airway via SeV vectors, for example, is at least 10-fold greater than that produced via AV vectors, and is 4- to 5-log-fold greater than that produced via cationic liposomes [Yonemitsu et al., 1996]. Finally, there is no evidence that SeV is pathogenic in humans. The SeV vector was designed using a rodent respiratory virus and has long been used for preparing hybridomas. In the retinal sensory system, an SeV vector produced high expression levels in retinal pigment epithelium after a brief vector-cell contact time, while AV did not [Ikeda et al., 2002]. Taken together, these data suggest that SeV might be a useful vector for delivering transgenes to other sensory systems, including the auditory system.

These properties make SeV vectors a prime candidate for the use in gene transfer therapy for treating hearing disorders. The aim of this study, therefore, was to evaluate the transfection efficiency of an SeV vector in the cochlea using two delivery pathways, the scala media and scala tympani.

Materials and Methods

Animals

We used 17 albino guinea pigs (250–350 g). All animal experiments were performed in accordance with the guidelines of the Keio University Committee for the Use and Care of Animals. The Keio University is fully accredited by the Association for Assessment and Accreditation of Laboratory Animal Care International.

Experimental Groups

We assigned animals to one of two groups: group 1 animals received either SeV (n = 6) or sterile artificial endolymph (NaCl 1 mM, KCl 126 mM, $KHCO_3$ 25 mM, $MgCl_2$ 0.025 mM, $CaCl_2$ 0.025 mM and K_2HPO_4 1.4 mM; n = 3) [Ishimoto et al., 2002] injections into the cochlea via the scala media, and group 2 animals received either SeV (n = 5) or perilymph (sterile normal Ringer's solution; n = 3) [Kanzaki et al., 2002b] injections into the cochlea via the scala tympani. SeV transfection efficacy was assessed histochemically. Auditory brain stem responses (ABRs) were measured before SeV injection and 3 days after injection, prior to sacrifice, to assess shifts in hearing threshold.

SeV Vectors

The full-length SeV genome contains the following: 3′-end leader followed by six viral genes – nucleocapsid, phospho, matrix, fusion (F), hemagglutinin-neuraminidase, and large proteins – and a small 5′-end trailer sequence (fig. 1). Since the F protein conveys viral infectivity, we used F gene-deleted SeV vectors (SeV/ΔF) in our experiments. SeV/ΔF do not produce infectious progeny [Li et al., 2000]. We constructed SeV/ΔF carrying green fluorescence protein (GFP-SeV/ΔF) as previously described [Li et al., 2000]. Briefly, GFP cDNA was amplified with a pair of *Not*I-tagged primers that contained the following SeV-specific transcriptional regulatory signal sequences: 5′-ATTGGCCGCCGTACGGCCATGGTGAGCAAGGGCGAGGAG-3′ and 5′-ATTGGCCGCCGTACGATGAACTTTCACCCTAAGTTTTTCTTACTTCGGAGCTTTACTTGTACAGCTCGTCCATGCCG-3′. A GFP-SeV/ΔF cDNA (pGFP-SeV/ΔF) was constructed by introducing the amplified fragment into the *Not*I site of the parental pSeV18+/ΔF. pGFP-SeV/ΔF was transfected into LLC-MK2 cells infected with vaccinia virus vTF7–3, which expresses T7 polymerase [Fuerst et al., 1986]. The T7-driven recombinant GFP-SeV/ΔF RNA genome was encapsulated by nucleocapsid, phospho, and large proteins, which were derived from their re-

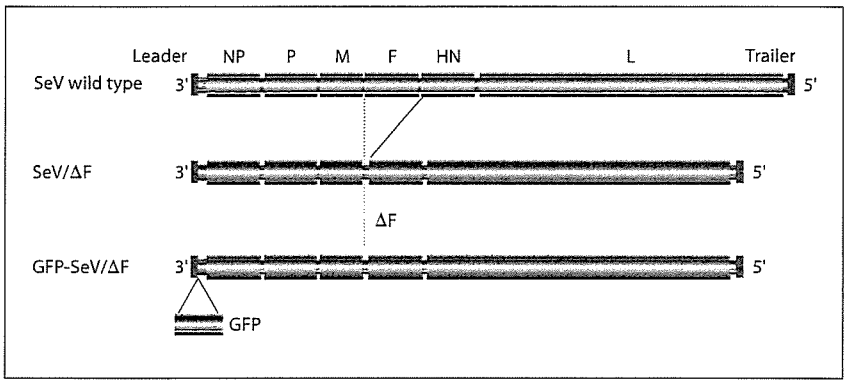

Fig. 1. The structures of the wild type of SeV, SeV/ΔF, and GFP-SeV/ΔF are shown. GFP-SeV/ΔF was used in this experiment. NP = Nucleocapsid; P = phospho; M = matrix; F = fusion; HN = hemagglutinin-neuraminidase; L = large proteins.

spective cotransfected plasmids. The recovered SeV vector was propagated using F protein-expressing packaging cell lines [Li et al., 2000]. Virus titers were determined, and infectivity was expressed as cell infectious units (CIU). The SeV vector was stored at –80°C until use.

Surgery

Guinea pigs were anesthetized with xylazine (10 mg/kg; i.m.) and ketamine HCl (40 mg/kg; i.m.). Prior to vector or control injections, 0.5 ml of 1% lidocaine HCl was injected subcutaneously around the ear as local anesthesia. GFP-SeV/ΔF (titer: 5×10^7 CIU/5 μl) was injected into the cochlea as described below.

In group 1 animals, the ventral side of the left bulla was opened, and a hole was drilled in the lateral wall of the third turn (fig. 2) as previously described [Ishimoto et al., 2002]. In group 2 animals, the left side of the middle ear was exposed via a postauricular approach. Under the guidance of an operating microscope, a small fenestra was made with a sharp probe in the otic capsule at the base of the cochlea [Prieskorn and Miller, 2000; Stover et al., 1999]. To inject SeV, we used a 100-μl Hamilton syringe with an attached vinyl cannula and fine polyamide tip. In group 1 animals, 5 μl of either GFP-SeV/ΔF or endolymph were injected into the scala media, and in group 2 animals, 5 μl of either GFP-SeV/ΔF or perilymph were injected into the scala tympani. Ten minutes after injection, the cannula was removed and the fenestra was covered with a small piece of fascia that adhered to the otic capsule. The bulla defect was sealed with carboxylate cement (Durelon® ESPE America, Norristown, Pa., USA). Dexon® adsorbable suture was used to close the subdermal opening, and nylon suture was used to close the skin opening.

ABR Measurement

A needle electrode was subdermally inserted at the vertex, along the dorsal midline of the scalp between the external auditory canals. The reference electrode was placed below the pinna of the left ear, and the ground electrode was inserted below the contralateral ear. The auditory stimulus consisted of a 1-ms tone burst with a rise-fall time of 0.1 ms. Waveforms from 256 stimuli were delivered at a frequency of 9 Hz. ABR waveforms were recorded for 12.8 ms, sampled at 40000 Hz, bandpass-filtered (50–5000 Hz), and averaged using PowerLab system software (PowerLab2/20, AD Instruments, Castle Hill, Australia). ABR waveforms were recorded in 5-dB SPL intervals from a maximum amplitude until no waveform could be observed. ABRs were recorded at 4, 12, and 16 kHz. The ABRs were measured with the animals under xylazine and ketamine anesthesia (i.m.). The researcher who measured ABRs was blinded to the animal's group assignment.

Statistical Analysis

Unpaired t tests were performed to test for significant differences in ABR thresholds at each frequency between the two groups. SPSS version 13.0 (Chicago, Ill., USA) was used.

Epifluorescent Stereoscopy

Animals were sacrificed under deep anesthesia 3 days after being injected with either vector or control solutions. To perfuse the inner and middle ears locally, we decapitated the animals and removed the temporal bone. The entire cochlea or lateral wall was visualized using a stereoscopic zoom microscope (SMZ1500) configured with epifluorescent optics (Nikon, Tokyo, Japan).

Immunohistochemistry

The cochlea was fixed in 4% paraformaldehyde, decalcified in 10% EDTA, and immersed in sucrose overnight for cryoprotection. After embedding in OCT compound [Whitlon et al., 2001], 10-μm-thick frozen sections were cut and collected. After permeabilization with 0.3% Triton X-100, the organ of Corti was stained for F-actin using a 1:100 solution of rhodamine phalloidin (Molecular Probes, Carlsbad, Calif., USA) for 30 min. The diluent for all solutions was PBS. Whole-mount preparations were observed using an Eclipse 80*i*® digital microscope configured with epifluorescent optics (Nikon).

Results

Transfection of the Cochlea after Injection into the Scala Media

GFP-positive cells were present in the cochlea and middle ear mucosa, including the otic capsule, of the ears receiving vector injections into the scala media

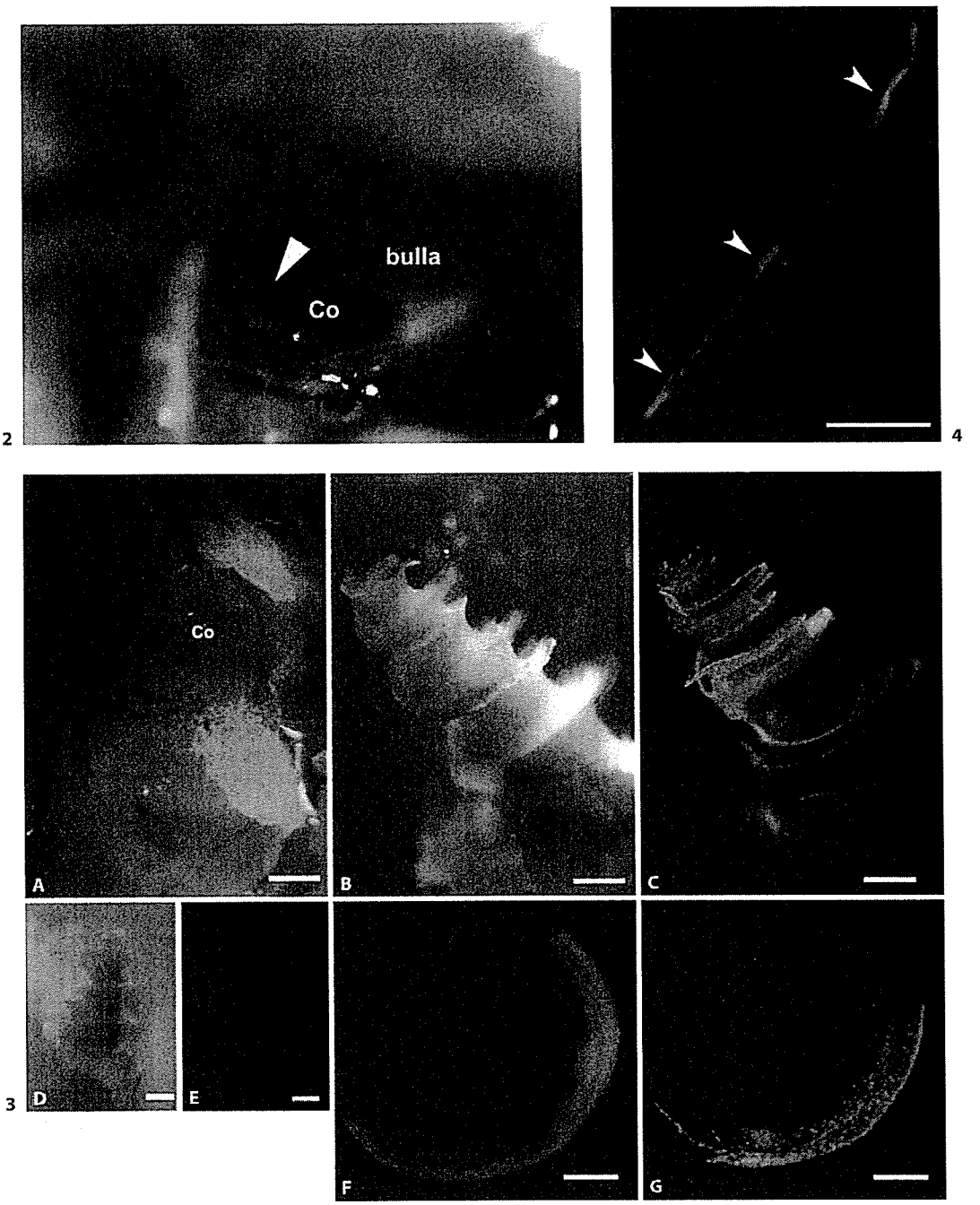

Fig. 2. Photomicrograph showing the surgical approach through the scala media. A ventrally located incision was made on the left ear, and then the window of the middle ear bulla was opened. A hole was made in the wall of the cochlear bone (arrowhead). Co = Cochlea; bulla = middle ear bulla.

Fig. 3. Photomicrographs of whole-mounted guinea pig cochlea showing the distribution of GFP-fusion protein after injection of GFP-SeV/ΔF into the scala media. **A** Fluorescent image showing the boney wall of the cochlea. **B**, **C** Light (**B**) and fluorescent (**C**) images of the cochlea of a SeV-inoculated ear. **D**, **E** Light (**D**) and fluorescent (**E**) images of the cochlea in an uninoculated, control ear. **F**, **G** Light (**F**) and fluorescent (**G**) images of the lateral wall of the inoculated ear. Scale bars:1000 μm (**A–E**);600 μm (**F**, **G**).

Fig. 4. Photomicrograph of histological section of guinea pig middle ear after injection of GFP-SeV/ΔF. GFP signal was observed in the middle ear mucosa (arrowheads). Scale bars: 10 μm.

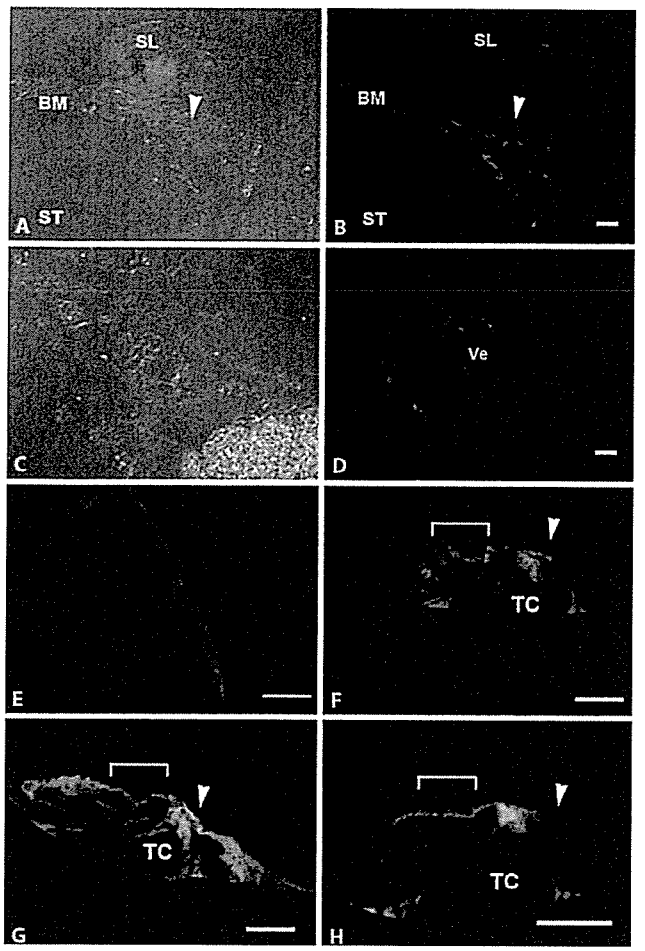

Fig. 5. Photomicrographs of histological sections of guinea pig scala media after injection of GFP-SeV/ΔF. **A**, **B** Spiral ganglion neuron (arrowhead); DIC image (**A**) and fluorescent image (**B**). **C**, **D** Cochlear blood vessel; DIC image (**C**) and fluorescent image (**D**). **E** Stria vascularis. **F–H** Organ of Corti with the arrowhead pointing to the inner hair cell and the bracket suggesting the outer hair cell region; the organ of Corti from an inoculated ear (**F**, **G**) and an uninoculated control ear (**H**). Red = F-actin stained with rhodamine phalloidin; green = GFP-SeV/ΔF-transfected cells; BM = basement membrane; SL = spiral limb; ST = scala tympani; TC = tunnel of Corti; Ve = cochlear blood vessel. Scale bars: 100 μm (**A–D**), 50 μm (**E**), 10 μm (**F–H**).

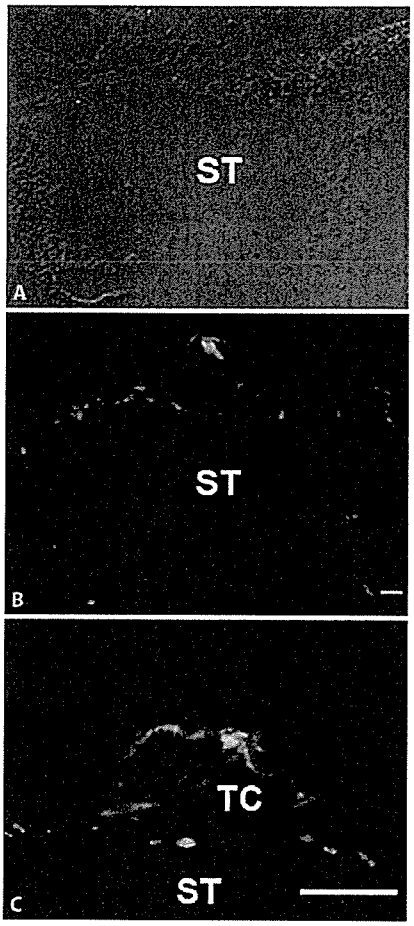

Fig. 6. The cochlea from an ear inoculated with GFP-SeV/ΔF via a scala tympani approach. **A–C** The organ of Corti and fibrocytes of the scala tympani; DIC image (**A**) and fluorescent image (**B**), and higher magnification (**C**); numerous labeled fibrocytes in the scala tympani. ST = Scala tympani; TC = tunnel of Corti. Scale bars: 100 μm (**A**, **B**), 10 μm (**C**).

(fig. 3A–C, fig. 4). This suggests that the injection leaked out of the cochlea and onto the middle ear mucosa. There were no GFP-positive cells in the contralateral ear (fig. 3D, E). GFP was also found in the lateral wall (fig. 3F, G). In one of the inoculated cochlea, GFP localized to several types of cells in several spiral ganglion neurons, in the outer layers of cochlear blood vessels and in the stria vascularis (fig. 5A–E). Transfected cells were found in the outer hair cell layer but not in the inner hair cell layer. In several animals, supporting cells (pillar, Hensen, Deiters, and Claudius cells) and inner and outer sulcus cells were also transfected (fig. 5F, G). We observed no GFP-positive cells in the uninoculated cochlea (fig. 5H).

Transfection of the Cochlea after Injection into the Scala Tympani

GFP-positive signals were found in many fibrocytes in the scala tympani of the inoculated ears (fig. 6A–C) but not in the contralateral or uninoculated ears (control)

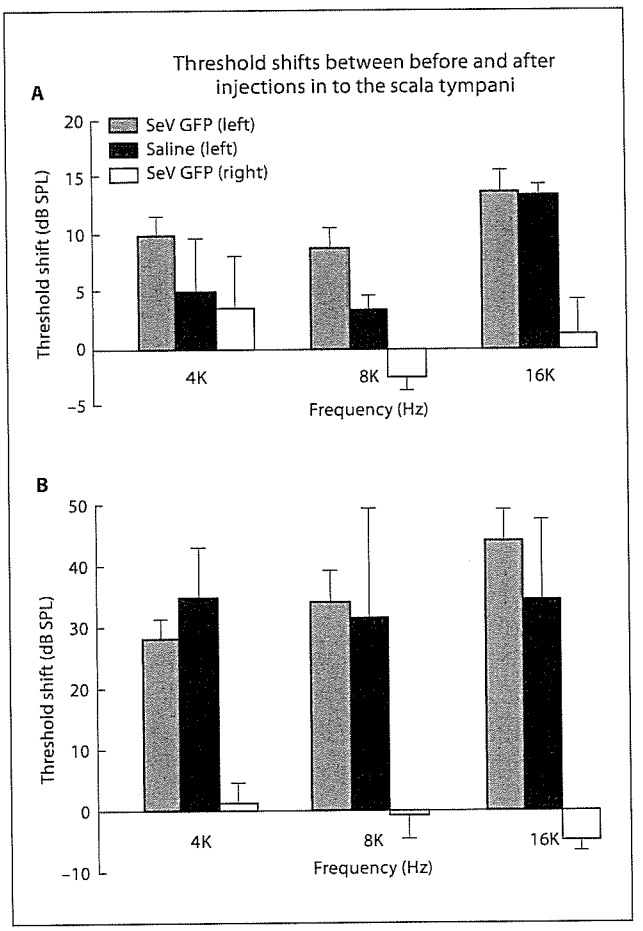

Fig. 7. ABR threshold shifts observed before and after injections via scala media (**A**) and scala tympani (**B**) approaches.

(data not shown). No GFP-positive cells were found in the scala media and vestibuli.

ABR Threshold Shift before and after Vector Injections

Hair cells disappeared in the animals that received SeV injections into the scala media. No obvious damage was seen, however, in the cochlea or middle ear of animals that received injections into the scala tympani. This is consistent with our ABR results, showing that pre- and postinjection threshold shifts were lower in animals operated through the scala tympani approach than in animals operated through the scala media approach. There were no statistically significant differences in hearing threshold shift among the animals that received SeV vector, endolymph, or perilymph injections, indicating that the SeV vector did not affect hearing function.

Table 1. Distribution of transgene expressions after SeV injection via scala media and tympani

Via scala media approach (n = 6)	Animals
Distribution of expression	
All (four) turns	3
Two turns	2
One turn	1
Site of expression	
Scala media	
Stria vascularis	2
Spiral ganglion neurons	1
Vessel	1
Reissner's membrane	1
Organ of Corti	
Inner hair cell	1
Outer hair cell	2
Pillar cells	2
Deiters cells	2
Hensen cells	6
Claudius cells	6
Inner sulcus cells	2
Scala tympani	
Fibrocytes	1
Via scala tympani approach (n = 5)	**Animals**
Distributions of expression	
All (four) turns	1
Two turns	2
One turn	2
Site of expression	
Scala tympani	
Fibrocytes	5

In group 1 (scala media approach), GFP-positive expressions were found at all turns (n = 3 ears), two turns (n = 2), and one turn (n = 1). GFP-positive transfection was found at a wide variety of cells at the scala media and tympani including the organ of Corti. In group 2 (scala tympani approach), GFP-positive expressions were found at all turns (n = 1), two turns (n = 2), and one turn (n = 1). GFP-positive transfection was found at numerous fibrocytes of the scala tympani but not scala media.

Discussion

Distribution of SeV-Transfected Cells

Our findings indicate that SeV vectors (5.0×10^7 CIU/5 μl) can efficiently transfer transgenes to a wide variety of cell types in the organ of Corti, including stria vascularis cells, spiral ganglion neurons (through scala media injections) and fibrocytes (through scala tympani injections) (table 1). The extent of SeV transfection is comparable to that obtained with AV vectors. When AV

vectors are injected into guinea pig cochlea at 1.0×10^{11} virus particles/ml (approximately 5.0×10^{8} virus particles/5 μl) via a scala media approach, AV vectors reach supporting cells such as interdental cells, inner sulcus cells, and Hensen cells [Ishimoto et al., 2002].

SeV may reach the sensory epithelial cells, spiral ganglion neurons, and stria vascularis by traversing the endolymphatic space and the lateral wall of the scala media. The route by which SeV vectors transfect spiral ganglion neurons is unknown. The vectors may penetrate the habenulae perforatae, in which the spiral ganglion nerve runs through a hole in the tympanic lip of the osseous spiral lamina. When injected via the scala tympani approach, SeV cannot penetrate the basement membrane and thus does not reach the organ of Corti as well as does AV.

SeV Does Not Affect Hearing Function

We find no significant differences in the hearing threshold of animals that received SeV, endolymph, or perilymph injections, indicating that SeV does not affect hearing function and that SeV may have lower levels of (cochlear) toxicity than do other viruses [Bitzer et al., 2003; Griesenbach et al., 2005]. We did find, however, that hearing function was differentially affected by the two routes of injection through the scala media and scala tympani. ABRs of animals operated via the scala tympani approach were lower than those of animals operated via the scala media approach. This disparity may be due to mechanical damage to the scala media. When AV is injected into the scala tympani, damage to auditory hair cells is limited [Han et al., 2004], whereas when it is injected into the scala media, numerous outer hair cell are damaged [Ishimoto et al., 2002]. This is consistent with our findings that injections into the scala media are more traumatic than injections into the scala tympani because injection via the scala media made pressure of endolymph followed by the rupture of Reissner's membrane which may mix cochlear fluid including perilymph and endolymph. Mixing fluids change Na^+ and K^+ ion in the inner ear and may not maintain homeostasis. The injection hole was also made in spiral ligament and stria vascularis and the direct flow pressed the organ of Corti through the tectorial membrane. This may be sufficient to damage hair cells.

Our data demonstrated that no GFP-positive expression was seen in the contralateral ear. Previous reports demonstrated that injection of 5 μl of AV vector did not transfect into the contralateral ear both via the scala tympani and media approach [Ishimoto et al., 2002]. However, Stover reported that 25 μl of AV was delivered to the contralateral ear [Ishimoto et al., 2002]. The distribution of transfection may depend on the amount of viral volume.

In conclusion, SeV may be useful for delivering a variety of therapeutic genes to the organ of Corti. Recent studies suggested that supporting cells can be induced to undergo mitosis and differentiate into hair cell phenotypes [Raphael, 1992]. Thus, SeV vectors can be used to promote hair cell regeneration by delivering gene products that induce differentiation of supporting cells to hair cells.

Our data demonstrate that SeV may be a powerful therapeutic tool for sensorineural hearing loss diseases to regenerate hair cells and may prevent spiral ganglion neuron degeneration.

Acknowledgements

We thank all the staff of DNAVEC Corporation, especially A. Tagawa, E. Suzuki and N. Kouno for their excellent technical assistance. This work is supported by grants from the Ministry of Health, Labor, and Welfare in Japan (S.K.).

References

Bitzer M, Armeanu S, Lauer UM, Neubert WJ: Sendai virus vectors as an emerging negative-strand RNA viral vector system. J Gene Med 2003;5:543–553.

Di Pasquale G, Rzadzinska A, Schneider ME, Bossis I, Chiorini JA, Kachar B: A novel bovine virus efficiently transduces inner ear neuroepithelial cells. Mol Ther 2005;11:849–855.

Fuerst TR, Niles EG, Studier FW, Moss B: Eukaryotic transient-expression system based on recombinant vaccinia virus that synthesizes bacteriophage T7 RNA polymerase. Proc Natl Acad Sci USA 1986;83:8122–8126.

Geschwind MD, Hartnick CJ, Liu W, Amat J, Van De Water TR, Federoff HJ: Defective HSV-1 vector expressing BDNF in auditory ganglia elicits neurite outgrowth: model for treatment of neuron loss following cochlear degeneration. Hum Gene Ther 1996;7:173–182.

Griesenbach U, Inoue M, Hasegawa M, Alton EW: Sendai virus for gene therapy and vaccination. Curr Opin Mol Ther 2005;7:346–352.

Han D, Yu Z, Fan E, Liu C, Liu S, Li Y, Liu Z: Morphology of auditory hair cells in guinea pig cochlea after transgene expression. Hear Res 2004;190:25–30.

Ikeda Y, Yonemitsu Y, Sakamoto T, Ishibashi T, Ueno H, Kato A, Nagai Y, Fukumura M, Inomata H, Hasegawa M, Sueishi K: Recombinant Sendai virus-mediated gene transfer into adult rat retinal tissue: efficient gene transfer by brief exposure. Exp Eye Res 2002; 75:39–48.

Inoue M, Tokusumi Y, Ban H, Shirakura M, Kanaya T, Yoshizaki M, Hironaka T, Nagai Y, Iida A, Hasegawa M: Recombinant Sendai virus vectors deleted in both the matrix and the fusion genes: efficient gene transfer with preferable properties. J Gene Med 2004;6: 1069–1081.

Ishimoto S, Kawamoto K, Kanzaki S, Raphael Y: Gene transfer into supporting cells of the organ of Corti. Hear Res 2002;173:187–197.

Izumikawa M, Minoda R, Kawamoto K, Abrashkin KA, Swiderski DL, Dolan DF, Brough DE, Raphael Y: Auditory hair cell replacement and hearing improvement by Atoh1 gene therapy in deaf mammals. Nat Med 2005;11:271–276.

Kanzaki S, Kawamoto K, Oh SH, Stover T, Suzuki M, Ishimoto S, Yagi M, Miller JM, Lomax M1, Raphael Y: From gene identification to gene therapy. Audiol Neurootol 2002a;7: 161–164.

Kanzaki S, Ogawa K, Camper SA, Raphael Y: Transgene expression in neonatal mouse inner ear explants mediated by first and advanced generation adenovirus vectors. Hear Res 2002b;169:112–120.

Kanzaki S, Stover T, Kawamoto K, Prieskorn DM, Altschuler RA, Miller JM, Raphael Y: Glial cell line-derived neurotrophic factor and chronic electrical stimulation prevent VIII cranial nerve degeneration following denervation. J Comp Neurol 2002c;454:350–360.

Kawamoto K, Ishimoto S, Minoda R, Brough DE, Raphael Y: Math1 gene transfer generates new cochlear hair cells in mature guinea pigs in vivo. J Neurosci 2003;23:4395–4400.

Kawamoto K, Sha SH, Minoda R, Izumikawa M, Kuriyama H, Schacht J, Raphael Y: Antioxidant gene therapy can protect hearing and hair cells from ototoxicity. Mol Ther 2004;9: 173–181.

Lalwani AK, Walsh BJ, Reilly PG, Muzyczka N, Mhatre AN: Development of in vivo gene therapy for hearing disorders: introduction of adeno-associated virus into the cochlea of the guinea pig. Gene Ther 1996;3:588–592.

Li HO, Zhu YF, Asakawa M, Kuma H, Hirata T, Ueda Y, Lee YS, Fukumura M, Iida A, Kato A, Nagai Y, Hasegawa M: A cytoplasmic RNA vector derived from nontransmissible Sendai virus with efficient gene transfer and expression. J Virol 2000;74:6564–6569.

Luebke AE, Steiger JD, Hodges BL, Amalfitano A: A modified adenovirus can transfect cochlear hair cells in vivo without compromising cochlear function. Gene Ther 2001;8: 789–794.

Masaki I, Yonemitsu Y, Komori K, Ueno H, Nakashima Y, Nakagawa K, Fukumura M, Kato A, Hasan MK, Nagai Y, Sugimachi K, Hasegawa M, Sueishi K: Recombinant Sendai virus-mediated gene transfer to vasculature: a new class of efficient gene transfer vector to the vascular system. FASEB J 2001;15:1294–1296.

Nakanishi M, Mizuguchia H, Ashihara K, Senda T, Akuta T, Okabe J, Nagoshi E, Masago A, Eguchi A, Suzuki Y, Inokuchi H, Watabe A, Ueda S, Hayakawa T, Mayumi T: Gene transfer vectors based on Sendai virus. J Control Release 1998;54:61–68.

Nazir SA, Metcalf JP: Innate immune response to adenovirus. J Investig Med 2005;53:292–304.

Prieskorn DM, Miller JM: Technical report: chronic and acute intracochlear infusion in rodents. Hear Res 2000;140:212–215.

Raphael Y: Evidence for supporting cell mitosis in response to acoustic trauma in the avian inner ear. J Neurocytol 1992;21:663–671.

Sakai Y, Kiyotani K, Fukumura M, Asakawa M, Kato A, Shioda T, Yoshida T, Tanaka A, Hasegawa M, Nagai Y: Accommodation of foreign genes into the Sendai virus genome: sizes of inserted genes and viral replication. FEBS Lett 1999;456:221–226.

Shiotani A, Fukumura M, Maeda M, Hou X, Inoue M, Kanamori T, Komaba S, Washizawa K, Fujikawa S, Yamamoto T, Kadono C, Watabe K, Fukuda H, Saito K, Sakai Y, Nagai Y, Kanzaki J, Hasegawa M: Skeletal muscle regeneration after insulin-like growth factor I gene transfer by recombinant Sendai virus vector. Gene Ther 2001;8:1043–1050.

Shirakura M, Inoue M, Fujikawa S, Washizawa K, Komaba S, Maeda M, Watabe K, Yoshikawa Y, Hasegawa M: Postischemic administration of Sendai virus vector carrying neurotrophic factor genes prevents delayed neuronal death in gerbils. Gene Ther 2004; 11:784–790.

Stover T, Yagi M, Raphael Y: Cochlear gene transfer: round window versus cochleostomy inoculation. Hear Res 1999;136:124–130.

Verma IM, Weitzman MD: Gene therapy: twenty-first century medicine. Annu Rev Biochem 2005;74:711–738.

Whitlon DS, Szakaly R, Greiner MA: Cryoembedding and sectioning of cochleas for immunocytochemistry and in situ hybridization. Brain Res Brain Res Protoc 2001;6: 159–166.

Yagi M, Kanzaki S, Kawamoto K, Shin B, Shah PP, Magal E, Sheng J, Raphael Y: Spiral ganglion neurons are protected from degeneration by GDNF gene therapy. J Assoc Res Otolaryngol 2000;1:315–325.

Yagi M, Magal E, Sheng Z, Ang KA, Raphael Y: Hair cell protection from aminoglycoside ototoxicity by adenovirus-mediated overexpression of glial cell line-derived neurotrophic factor. Hum Gene Ther 1999;10:813–823.

Yonemitsu Y, Kaneda Y, Morishita R, Nakagawa K, Nakashima Y, Sueishi K: Characterization of in vivo gene transfer into the arterial wall mediated by the Sendai virus (hemagglutinating virus of Japan) liposomes: an effective tool for the in vivo study of arterial diseases. Lab Invest 1996;75:313–323.

Yonemitsu Y, Kitson C, Ferrari S, Farley R, Griesenbach U, Judd D, Steel R, Scheid P, Zhu J, Jeffery PK, Kato A, Hasan MK, Nagai Y, Masaki I, Fukumura M, Hasegawa M, Geddes DM, Alton EW: Efficient gene transfer to airway epithelium using recombinant Sendai virus. Nat Biotechnol 2000;18:970–973.

Available online at www.sciencedirect.com
SCIENCE DIRECT
Hearing Research 214 (2006) 28–36
Hearing Research
www.elsevier.com/locate/heares

Research paper

$p27^{Kip1}$ deficiency causes organ of Corti pathology and hearing loss

Sho Kanzaki [b], Lisa A. Beyer [a], Donald L. Swiderski [a], Masahiko Izumikawa [a], Timo Stöver [c], Kohei Kawamoto [d], Yehoash Raphael [a,*]

[a] *Kresge Hearing Research Institute, The University of Michigan Medical School, MSRB III Room-9303, 1150 West Medical Center Drive, Ann Arbor, MI 48109-0648, USA*
[b] *Department of Otolaryngology, Keio University, 35 Shinanomachi, Shinjuku, Tokyo 160-0016, Japan*
[c] *Department of Otolaryngology, Hannover University, Germany*
[d] *Department of Otolaryngology, Kansai Medical University, Osaka, Japan*

Received 30 June 2005; received in revised form 30 December 2005; accepted 18 January 2006
Available online 2 March 2006

Abstract

$p27^{Kip1}$ (p27) has been shown to inhibit several cyclin-dependent kinase molecules and to play a central role in regulating entry into the cell cycle. Once hair cells in the cochlea are formed, p27 is expressed in non-sensory cells of the organ of Corti and prevents their re-entry into the cell cycle. In one line of p27 deficient mice ($p27^{-/-}$), cell division in the organ of Corti continues past its normal embryonic time, leading to continual production of cells in the organ of Corti. Here we report on the structure and function of the inner ear in another line of p27 deficient mice originating from the Memorial Sloan-Kettering Cancer Center. The deficiency in p27 expression of these mice is incomplete, as they retain expression of amino acids 52–197. We determined that mice homozygote for this mutation had severe hearing loss and their organ of Corti exhibited an increase in the number of inner and outer hair cells. There also was a marked increase in the number of supporting cells, with severe pathologies in pillar cells. These data show similarities between this $p27^{Kip1}$ mutation and another, previously reported null allele of this gene, and suggest that reducing the inhibition on the cell cycle in the organ of Corti leads to pathology and dysfunction. Manipulations to regulate the time and place of p27 inhibition will be necessary for inducing functionally useful hair cell regeneration.

Keywords: Hair cell; Cell cycle; Deafness; $p27^{Kip1}$; Mouse

1. Introduction

During embryonic development of the mouse cochlea, the transition from the proliferative stage to the period of hair cell differentiation starts around embryonic day (E) 13 (Chen and Segil, 1999; Lumpkin et al., 2003; Ruben, 1967; Woods et al., 2004). In normal mice, no new cells are added to the sensory epithelium after embryonic day 15. Several cell-cycle regulating proteins have been shown to participate in the transition from proliferation to differentiation. The genes encoding these proteins include $p27^{Kip1}$ (p27), a member of the Cip–Kip family of cyclin-dependent kinases (Chen and Segil, 1999; Lowenheim et al., 1999), Ink4d (Chen et al., 2003) and the retinoblastoma gene Rb1, a tumor suppressor gene (Sage et al., 2005). Other genes that have not yet been identified may also be involved. Better understanding of the gene expression cascade leading to cell-cycle quiescence in the organ of Corti may be instrumental in finding ways to manipulate the cell cycle in this organ and design ways to induce generation of new hair cells to repopulate the deafened organ of Corti.

A previous study found that p27 is an important regulator of progenitor cell proliferation during development of the brain, retina and other tissues (Assoian, 2004). p27 was found to be upregulated during the late G2 or early G1 phase of the cell cycle (Koff and Polyak, 1995). Over-expression of

* Corresponding author. Tel.: +1 734 936 9386; fax: +1 734 615 8111/647 2563.
E-mail address: yoash@umich.edu (Y. Raphael).

0378-5955/$ - see front matter © 2006 Elsevier B.V. All rights reserved.
doi:10.1016/j.heares.2006.01.014

p27 in progenitor cells leads to their premature exit from the cell cycle (Tarui et al., 2005). A complete deletion of the gene leads to gigantism and excess proliferation in several tissues including hematopoietic, pituitary and ovarian cells (Fero et al., 1996). In the cochlea of mice lacking one or both alleles of p27, the proportion of mitotic cells in the cochlea is increased (Chen and Segil, 1999; Lowenheim et al., 1999). These mice exhibit excessive number of cells in the organ of Corti (Chen and Segil, 1999; Lowenheim et al., 1999) and impaired hearing (Lowenheim et al., 1999).

The deletion studies mentioned above examined the effects of a complete deletion of the gene (Fero et al., 1996; Nakayama et al., 1996). In this study, we examine the effects of a less severe mutation generated at the Memorial Sloan-Kettering Cancer Center (Kiyokawa et al., 1996). This mutation is a partial deletion eliminating the first 51 amino acids, resulting in a hypomorphic allele with reduced ability to inhibit cyclin-dependent kinase activity (Kiyokawa et al., 1996). Our goal was to characterize the inner ear phenotype of transgenic mice with this incomplete p27 deficiency. Using acoustic brainstem response (ABR) audiometry, we determined that their hearing is severely impaired. Using SEM, TEM and cytochemistry, we determined that the sensory epithelium has pathological changes in both hair cells and supporting cells.

2. Materials and methods

2.1. Animals and genotype analysis

p27 deficient mice (Kiyokawa et al., 1996) were kindly provided by Dr. Koff (The Memorial Sloan-Kettering Cancer Center, NY). The genetic background of these mice was hybrid 129SvJ with C57Bl/6. The three different genotypes used were $p27^{+/+}$ (wild-type, normal control $N = 4$), $P27^{+/-}$ (heterozygous $N = 5$) and $P27^{-/-}$ (homozygous for the p27 deficiency $N = 5$). Animal care and handling were approved by the University of Michigan Institutional Committee on the Use and Care of Animals and were performed using accepted veterinary standards. Mice were sacrificed at the age of 21 days (P21) and genotyped by PCR using tail DNA as previously reported (Kiyokawa et al., 1996), with the following DNA fragments: 294, 61 (bp) for $P27^{-/-}$, 294, 223, 71, 61 (bp) for $P27^{+/-}$, 223, 71 (bp) for wild-types.

2.2. ABR analysis

To assess ABR thresholds, mice ($P27^{-/-}$ $N = 3$; $P27^{+/-}$ $N = 3$, and $p27^{+/+}$ $N = 2$) were tested at 4, 10 and 20 kHz. Animals were anesthetized with mixture of xylazine (1.25 mg/g) and ketamine (62.5 mg/g). An active needle electrode was subdermally inserted at the vertex, along the dorsal midline of the scalp between the external auditory canals. The reference electrode was placed below the pinna of the left ear and the ground electrode was inserted below the contralateral ear.

The sound stimulus consisted of a 15 ms tone burst with rise–fall time of 1 ms. The sound stimuli were delivered from an encased, shielded Beyer earphone through a 13 mm tube into the ear canal. Response waveforms (100,000 gain, filtered from 0.3 to 3 kHz) were averaged (1024 epochs) using a Tucker Davis data acquisition system. The response threshold was defined as the interpolated value between the last level in which a response was presented and 5 dB lower where no response was observed.

We performed ANOVA to test for differences in ABR thresholds among the three genotypes at each frequency. Because three frequencies were tested, we used a Bonferroni-adjusted critical p-value of 0.015. When the ANOVA found a significant difference, unpaired t-tests were used to determine which genotypes were significantly different, again using a Bonferroni-adjusted critical p-value of 0.015.

2.3. Scanning electron microscopy (SEM)

We used two 21-day old animals from each genotype ($P27^{-/-}$, $P27^{+/-}$ and $p27^{+/+}$). Animals were anesthetized and perfused with 2% paraformaldehyde and 2% glutaraldehyde in 0.15 M cacodylate. Cochleae were removed and fixed in the same fixative overnight. Tissues were then incubated in 1% osmium tetroxide for 60 min. Samples were dehydrated in ethanol and critical point dried with CO_2 in a SamDri 790 (Tousimis, Rockville, MD). Samples were mounted on stubs, sputter coated with gold using Polaron 5100 (Polaron Equipment Limited, Watford Hertfordshire, UK) and examined on a Phillips FEI XL30FEG SEM. The entire cochlear length was analyzed and the images presented are from the lower apical turn.

2.4. Transmission electron microscopy (TEM)

Cochleae from two mice of each phenotype ($P27^{-/-}$, $P27^{+/-}$ and $p27^{+/+}$) were used. Animals were anesthetized and perfused with 2% paraformaldehyde and 2% glutaraldehyde in 0.15M cacodylate. Cochleae were removed, osmicated (as above) and decalcified until soft (approximately one week). Tissues were stained with aqueous uranyl acetate, dehydrated in ethanol followed by propylene oxide, and embedded in Embed 812 epoxy resin (Electron Microscopy Sciences, Washington, PA). Epon blocks were sectioned using a Leica Ultracut R ultramicrotome using a diamond knife (slice thickness; 80 nm). Sections from the lower apical turn were collected on grids (Electron Microscope Sciences, 200 Hex mesh T/B). The grids were stained with uranyl acetate and lead citrate and examined on a Phillips CM 100 TEM.

2.5. Whole-mount analysis

We used a phalloidin stain to label F-actin in the tissue in order to enhance identification of cell types and their organization in the sensory epithelium (Raphael et al.,

1994b) and Hoechst to stain DNA and visualize nuclei (Raphael, 1993). Animals (three from each genotype) were deeply anesthetized, decapitated, and their temporal bones were removed. The cochleae were excised, the bony capsule removed and tissues were fixed in 4% paraformaldehyde for 2 h. Further dissection was performed to remove the lateral wall tissues and the tectorial membrane. The samples were permeabilized with 0.3% Triton X-100 in PBS for 5 min, and incubated for 30 min in rhodamine conjugated phalloidin (Jackson Immunoresearch, West grove, PA) diluted 1:100 in PBS. Stained whole-mount of the apical turn were mounted on microscope slides with Crystal/Mount (Biomedia, Foster City, CA), and examined with a laser scanning confocal microscope (BioRad MRC600) with a 63 × N/A 1.4 objective attached to Nikon Diaphot microscope. Z-series images (1 μm interval) were taken at the lower apical turn, starting from the apical luminal aspect of the sensory epithelium, spanning the entire epithelial layer and terminating at the extracellular matrix beneath the epithelium. Files were converted and stored as TIFF files. The Z-series stack was then converted to individual image files using NIH Image.

Two ears of each genotype were also stained with Hoechst 33342 (Molecular Probes, Eugene, OR) and photographed with epi-fluorescence (Leica DMRB upright photomicroscope) at several focal planes. Images at the UV wavelength were obtained from the lower apical turn with a digital monochrome Spot camera (Diagnostic Instruments, Inc., Sterling Heights, MI). The number of nuclei in the outer hair cell area was counted in all focal planes of the epithelium.

2.6. Image processing

We used Adobe Photoshop for adjustment of image contrast, insert symbols and letters for labels and crop images for preparation of figure panels.

3. Results

Confocal microscopy images of phalloidin stained whole-mounts of the organ of Corti reveals that the homozygous mutant mouse ($p27^{-/-}$) has hair cells and supporting cells, but that their organization and appearance are abnormal (Fig. 1A). In several locations along the cochlear duct, two rows of inner hair cells and four rows of outer hair cells were observed, rather than the normal one and three rows, respectively. The morphology of the supporting cells in $p27^{-/-}$ is also abnormal. This is most evident in the pillar cells, where the thick actin filaments near the apical surfaces of the cells are disorganized. In heterozygotes ($p27^{+/-}$, Fig. 1B), the organization of the mosaic of the auditory epithelium is much closer to that seen in the wild-type ($p27^{+/+}$, Fig. 1C). The $p27^{+/-}$ mice display a nearly normal organization of hair cells, but the junctional actin in supporting cells is slightly altered, especially in pillar cells. In wild-type animals (Fig. 1C) the organization of the pillar cells and the rows of hair cells is regular and the number of cells in each row is usually constant, with one row of inner hair cells and three rows of outer hair cells.

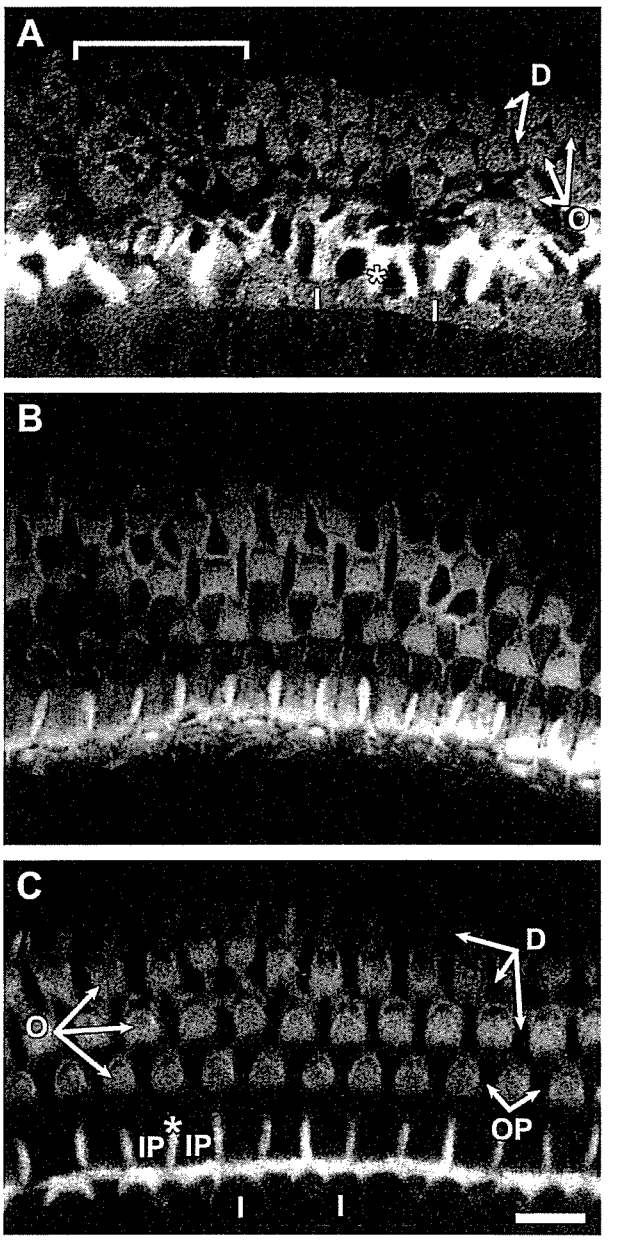

Fig. 1. Confocal microscopic images of phalloidin stained whole-mounts of the organ of Corti from $p27^{-/-}$ homozygouse mutant (A), $p27^{+/-}$ heterozygous (B) and $p27^{+/+}$ wild-type (C) mice. A: Several outer hair cells are missing (bracket). Remaining outer hair cells (O arrows point to outer hair cell rows 1–3) are in disarray. The actin bundles which represent intercellular junctions between inner pillar cells reveal disorganization of the apical portions of pillar cells (asterisk). The typical dumbbell shape of the Deiters cell apical surface is abnormal (D arrows). I denotes inner hair cells. B: Outer hair cell and pillar cells are closer to normal but their organization is imperfect. C: Actin bundles depict the typical normal organization of hair cells and supporting cells of the organ of Corti. D arrows point to three rows of Deiters cells, O arrows point to three rows of outer hair cells, OP point to outer pillar cells, IP denotes inner pillar, asterisk points to the junctional actin between inner pillar cells, I marks inner hair cell. Scale bar: 10 μm.

The nuclei of the auditory epithelium were analyzed in whole-mounts of the organ of Corti of wild-type and $p27^{-/-}$ animals. Nuclei in the outer hair cell area of the normal organ of Corti are round and arranged in clear and distinctive three rows, visible beneath the luminal surface (Fig. 2). Immediately beneath the three rows of outer hair cell nuclei, are the Deiters cell nuclei. Moving further towards the basilar membrane reveals a dense aggregation of spindle-shaped nuclei representing mesothelial cells residing underneath the epithelium, lining the scala tympani (Fig. 2D). Thus, two distinct rows of nuclei are observed above the mesothelial layer in the outer hair cell area of the normal cochlea. In the $p27^{-/-}$ mutant ears (Fig. 3), hair cell nuclei were seen in three rows of that were somewhat less well organized than in the normal ear (Fig. 3B, compare to Fig. 2B). The contour of the nuclei was nearly round but many nuclei showed slightly distorted shape (Fig. 3B). When observing lower focal planes (towards the basilar membrane), the $p27^{-/-}$ ear contained numerous nuclei at all focal planes under the luminal surface (Fig. 3C–E). Thus, nuclei in the Deiters cell area appeared to be present at more than one focal plane.

Nuclei were counted in an area measuring 50×50 μm in the outer hair cell region. Counts in three such areas averaged a total of 43 nuclei in the wild-type animals versus 68 nuclei in $p27^{-/-}$ animals, representing an increase of more than 50%. Because some hair cell loss is already apparent at this age, we infer that the increase in the number of nuclei represents mostly an increase in the number of supporting cells (Fig. 1A).

SEM confirms the presence of supernumerary hair cells and disorganized apical surface of supporting cells (Fig. 4). In the $p27^{-/-}$ ears, the normal organization of pillar and Deiters cells could not be observed (Fig. 4A). The $p27^{+/-}$ ears (Fig. 4B) exhibited an intermediate phenotype between the wild-type and the $p27^{-/-}$ ears. Individual hair cells did not appear perfectly normal in the mutant animals (Fig. 5) but the differences between normal wild-type ears and mutants was not as marked as that seen in supporting cells.

In cross sections, no tunnel of Corti or Nuel space are observed (Fig. 6). Instead, numerous cells occupy these

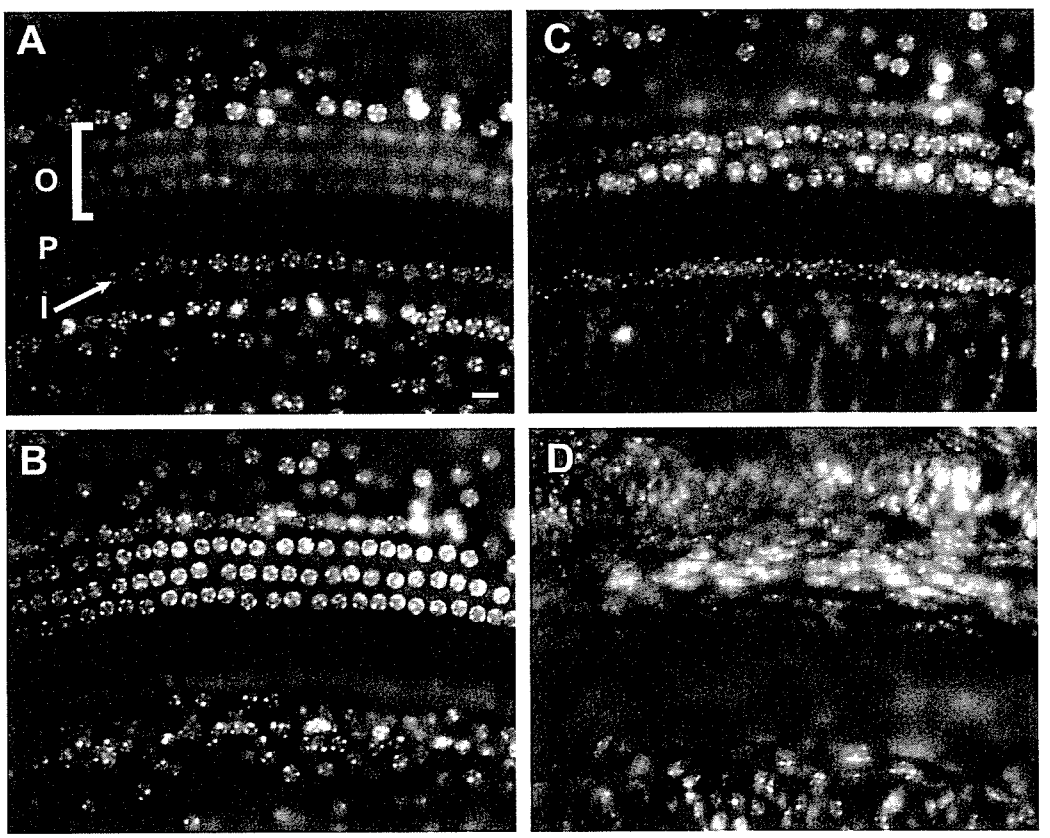

Fig. 2. The normal organ of Corti contains two distinctive planes of nuclei in the outer hair cell area. Whole-mounts of the organ of Corti of a wild-type $p27^{+/+}$ mouse stained with Hoechst and photographed at four focal planes starting above the nuclei of outer hair cells (A) and descending towards the area under the basilar membrane (D). A: nuclei of inner hair cells (I) and Hensen cells (at upper end of bracket) flank the outer hair cell area above the focal plane of outer hair cell nuclei (P shows area of pillar cell heads). B: Outer hair cell nuclei are arranged in three distinctive and well organized rows. The perimeter of outer hair cell nuclei is round and smooth. C: At a lower focal plane, nuclei of Deiters cells (supporting cell) are clearly identified. Nuclei of these cells are slightly larger than outer hair cell nuclei. D: The next set of nuclei visible under the Deiters cell nuclei are spindle-shaped nuclei of mesothelial cells residing under the basilar membrane. Scale bar (in A, for A–D): 10 μm.

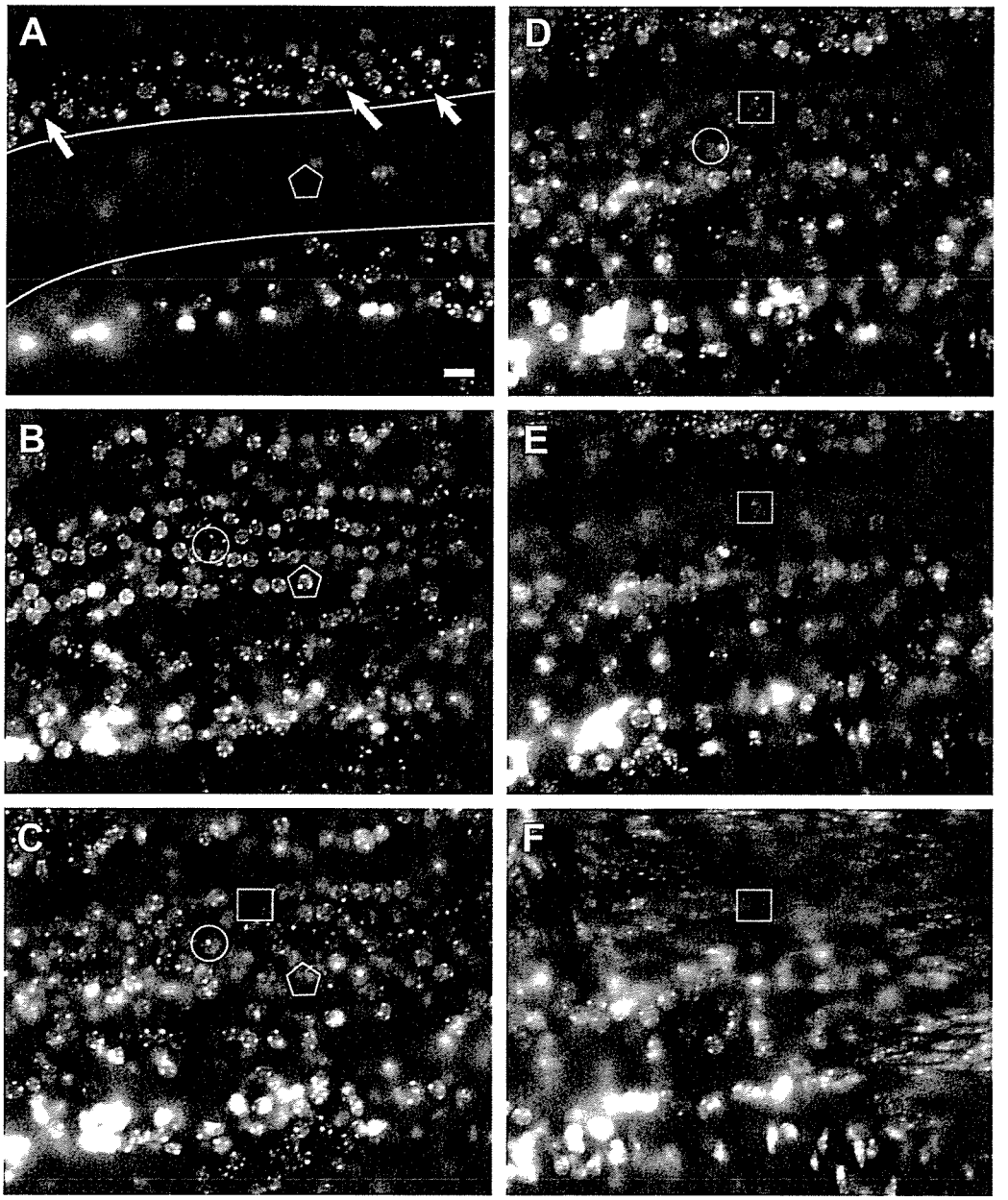

Fig. 3. In the outer hair cell area of $p27^{-/-}$ mice the nuclei are spread throughout the epithelium at all focal planes, as depicted by Hoechst stained whole-mount photographed at six different planes (A–F) from just under the luminal surface (A) to under the basilar membrane (F). A: Immediately beneath the luminal surface there are no visible nuclei in the outer hair cell area (between the border lines) but Hensen cell nuclei are seen in the lateral aspect of the organ of Corti (arrows) and inner hair cell nuclei are in the medial side. The pentagon is a selected area with no nucleus, corresponding the nucleus present in B. B: Outer hair cell nuclei appear at a lower focal plane. The perimeter of the nuclei is slightly rough and the spherical shape is less well defined than in normal mice (compare to Fig. 2B). The circle depicts an area with no nucleus, corresponding to the area in C where a nucleus appears. C: Numerous supporting cell nuclei are visible under the level of the outer hair cell nuclei. Supporting cell nuclei are slightly larger than outer hair cell nuclei. The square introduces an area devoid of a nucleus, in which a lower focal plane will contain a nucleus (in D). D: Many additional supporting cell nuclei are seen in a lower focal plane. E: A lower focal plane in which most nuclei shown in D disappear, and others appear. This is the lowest focal plane in the epithelium, immediately above the basilar membrane. F: Spindle shape nuclei (mesothelial cell nuclei) appear at a lower focal plane just beneath the basilar membrane. Scale bar (in A, for A–F): 10 μm.

fluid spaces (Fig. 6A). These cells could be pillar cells and Deiters cells and/or progenitor cells that are in the process of differentiating or dividing. The morphology of outer hair cells is pathological (Fig. 6A) but inner hair cells appear relatively normal (Fig. 6A and B). Supporting cell nuclei are not restricted to a single focal plane below the row of outer hair cell nuclei, but instead, they are observed in multiple levels in the epithelium (Fig. 6A, compare to Fig. 3C–E). Some of the supporting cell nuclei reside in the basal region of the epithelium, adjacent to the basilar

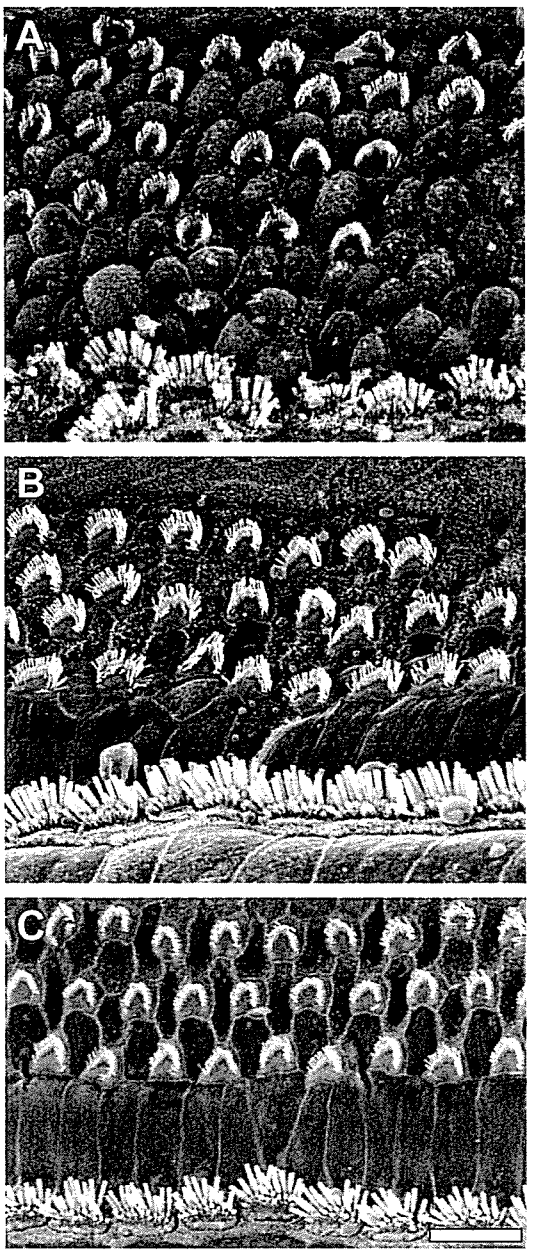

Fig. 4. SEM micrographs of the surface of the auditory epithelium in $p27^{-/-}$ (A), $p27^{+/-}$ (B) and $p27^{+/+}$ (C) mice. A: Inner hair cells are not well organized and a few of them form a second row. Outer hair cells are poorly organized and four rows can be discerned. The surface of supporting cells between outer hair cells is wider than usual and the cell borders are abnormal. The surface of the pillar cells has many more cells than in normal ears and lacks clear organization. B: The appearance of hair cells and supporting cells is close to normal. The number of cell rows is normal in both inner and outer hair cells. Pillar cell organization is slightly imperfect. C: The morphology of hair cells and supporting cells is normal. Magnification bar: 10 μm.

membrane. These nuclei appear to be attached to the basal lamina and flatten against it (Fig. 6A).

ABR audiometry (Fig. 7) shows that homozygous $p27^{-/-}$ mice have severe hearing loss at the three tested frequencies (4, 10 and 20 kHz) whereas heterozygous mice are much closer to wild-type, which exhibit normal hearing. ANOVA indicates that there are statistical differences in ABR thresholds among genotypes at each frequency. *T*-tests indicate that homozygous mutants have significantly higher thresholds than heterozygotes at each frequency. Although heterozygotes tend to have higher thresholds than wild-types, the differences were not significant at any of the tested frequencies.

4. Discussion

Overall, the structure and function of the inner ears of mice described in this report are similar to previous reports of different p27 mutations. We found that auditory function is severely impaired in $p27^{-/-}$ mice, and appears to be slightly impaired in the heterozygotes. The morphology of the sensory epithelium is consistent with the functional data and follows a similar hierarchy of pathology. Hair cells were present in all three genotypes and the most prominent pathology appeared to be in the number and organization of supporting cells.

The functional deficit in the $p27^{-/-}$ mice may be related to more than one pathology. The irregular organization of the outer hair cell area is incompatible with a normal "active" cochlea. As such, a threshold shift of 50–60 dB is expected due to the outer hair cell pathology (Dallos and Harris, 1978). In addition, it is likely that differentiation of the inner hair cells is incomplete due to crowding. Because the mosaic organization of the organ of Corti is dependent on both cell types, it is difficult to determine which cell is responsible for the primary pathology. Furthermore, p27 has a role in normal differentiation of neuronal tissues (Baldassarre et al., 2000; Sasaki et al., 2000), so the innervation of the auditory hair cells in p27 deficient mice also is likely to be abnormal.

The data obtained from cross sections of the $p27^{-/-}$ organ of Corti suggest that the excess in cell number is more prominent in supporting cells. The observation that some supporting cell nuclei are positioned flat against the basilar membrane indicates that these cells may be in s-phase, as previously shown in the regenerating auditory epithelium of birds (Raphael et al., 1994a). This suggests that new cells are still being added to the epithelium in these 21-day-old mice, more than four weeks after mitosis in the sensory epithelium is normally completed. It is possible that some of these newly-added cells differentiate into new hair cells.

Mice homozygous for the other p27 mutation (Nakayama et al., 1996) are also severely hearing impaired (Lowenheim et al., 1999), yet the pathology is not identical to that in the mouse we now describe. The organ of Corti of both p27 mutants is disorganized and includes supernumerary supporting cells and hair cells. The pathology and hearing impairment are severe in homozygotes of both mutants, but the heterozygotes seem to be slightly different. Elevated thresholds are seen in the heterozygotes of the partially deleted gene (hypomorphic mutation reported

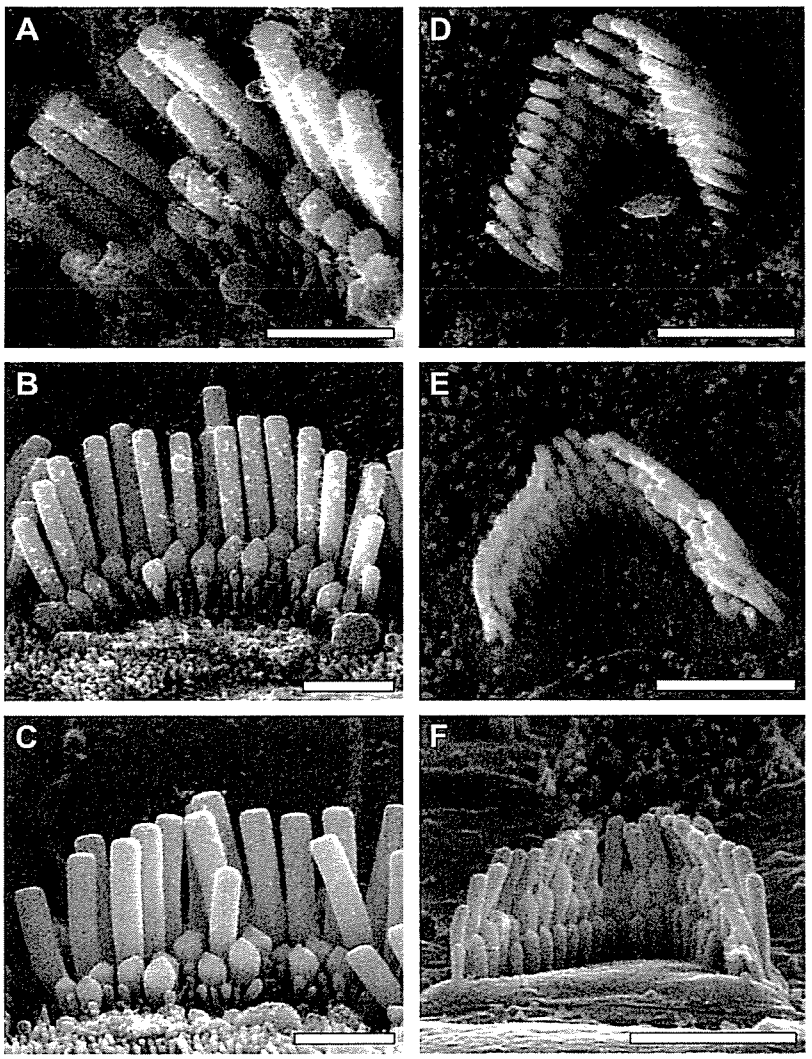

Fig. 5. SEM of apical surface of inner hair cells (A–C) and outer hair cells (D–F) of $p27^{-/-}$ (A and D), $p27^{+/-}$ (B and E) and $p27^{+/+}$ mice (C and F). The number, height and organization of stereocilia are similar in all three genotypes, but $p27^{-/-}$ hair cells appear to have slightly disorganized stereocilia, especially on the inner hair cell. Scale bars: 2 μm.

here) but not in the heterozygotes of the completely deleted p27 gene (Lowenheim et al., 1999). We speculate that the slight hearing loss in the heterozygotes of the hypomorphic deletion (studied here) is due to a dominant negative role assumed by the truncated protein in the organ of Corti. Reduced compensatory role of other genes may also play a role in the pathology seen in the hypomorphic deletion. Another possibility is that the genetic background of these hybrid mice plays a role in the severity of the heterozygote phenotype.

The genetic background of the $p27^{Kip1}$ mutant animals used in this study was hybrid 129SvJ with C57Bl/6. Both strains carry a synonymous single-nucleotide polymorphism (SNP) in exon 7 of *Cdh23* that is significantly associated with *Ahl* (Noben-Trauth et al., 2003). However, mice used in this study were 21 days old, much younger than the expected onset of age-related hearing loss, thus the pathology they exhibit is likely independent of *Ahl*.

Although the unregulated production of cells in the organ of Corti appears to involve a functional deficit, the results do have implications for designing controlled methods for inducing hair cell regeneration in the mammalian cochlea. A better understanding of cell cycle regulation in the organ of Corti may lead to enhanced ability to manipulate the genes involved in this process. Regulated inhibition of p27, Rb1 (Sage et al., 2005) or other cell cycle proteins may produce a pulse of cell generation that can be used for reconstructing the pathological organ of Corti. Skp2, a F-box protein that can inhibit p27 by unbiquitination, is present in the inner ear (Dong et al., 2003) and may be used to regulate the levels of p27. To accomplish functionally meaningful hair cell regeneration, it may also be necessary to combine the manipulation of cell cycle with induction of hair cell differentiation by genes such as *Atoh1* (Bermingham et al., 1999; Izumikawa et al., 2005; Shou et al., 2003).

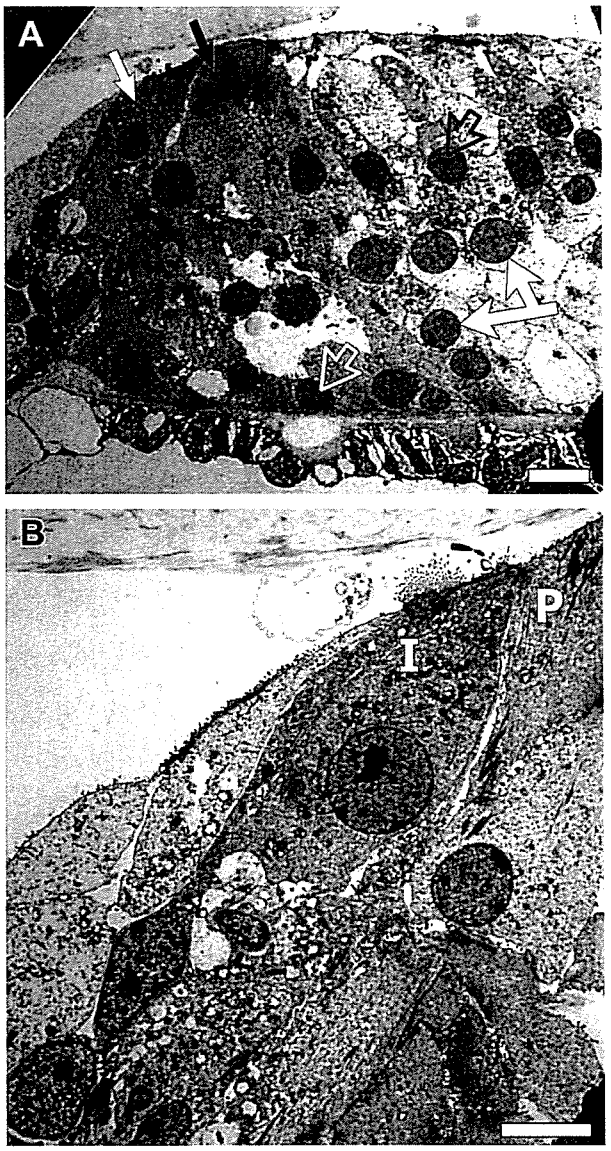

Fig. 6. TEM micrographs of organ of Corti sections in $p27^{-/-}$ cochleae. A: The inner hair cell (white filled arrow) has relatively normal morphology. Outer hair cells nuclei are present (black open arrow) but the cells bodies are pathological. Pillar cell (black filled arrow) morphology in the apical domain is abnormal, and the basal domain is not clearly identified. Supporting cell nuclei appear under the outer hair cells (double arrow) and in additional locations, including close proximity to the basilar membrane. One nucleus is flattened against the basal lamina (white open arrow). B: An inner hair cell (I) with relatively normal morphology. The adjacent pillar cell (P) appears undifferentiated and lacks typical pillar shape and cytoskeletal components. Scale bars: 10 μm in A and 5 μm in B.

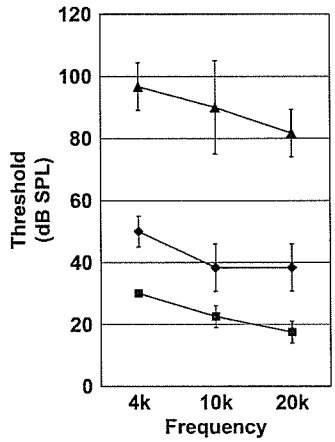

Fig. 7. ABR thresholds for the three genotypes in each of the three tested frequencies. Data points represent the mean thresholds and standard deviation. Squares are for $p27^{+/+}$, diamonds represent $p27^{+/-}$ and triangles for $p27^{-/-}$.

Acknowledgements

We thank Graham Atkin for technical assistance. This work was supported by Berte and Alan Hirschfield, the CHD, GM and the UAW, a grant from the Japan Ministry of Health and Labor H16-008, and NIH NIDCD Grants R01-DC05053 and R01-DC01634 and P30 DC05188.

References

Assoian, R.K., 2004. Stopping and going with p27kip1. Dev Cell 6, 458–459.

Baldassarre, G., Boccia, A., Bruni, P., Sandomenico, C., Barone, M.V., Pepe, S., Angrisano, T., Belletti, B., Motti, M.L., Fusco, A., Viglietto, G., 2000. Retinoic acid induces neuronal differentiation of embryonal carcinoma cells by reducing proteasome-dependent proteolysis of the cyclin-dependent inhibitor p27. Cell Growth Differ. 11, 517–526.

Bermingham, N.A., Hassan, B.A., Price, S.D., Vollrath, M.A., Ben-Arie, N., Eatock, R.A., Bellen, H.J., Lysakowski, A., Zoghbi, H.Y., 1999. Math1: an essential gene for the generation of inner ear hair cells. Science 284, 1837–1841.

Chen, P., Segil, N., 1999. p27(Kip1) links cell proliferation to morphogenesis in the developing organ of Corti. Development 126, 1581–1590.

Chen, P., Zindy, F., Abdala, C., Liu, F., Li, X., Roussel, M.F., Segil, N., 2003. Progressive hearing loss in mice lacking the cyclin-dependent kinase inhibitor Ink4d. Nat. Cell Biol. 5, 422–426.

Dallos, P., Harris, D., 1978. Properties of auditory nerve responses in absence of outer hair cells. J. Neurophysiol. 41, 365–383.

Dong, Y., Nakagawa, T., Endo, T., Kim, T.S., Iguchi, F., Yamamoto, N., Naito, Y., Ito, J., 2003. Role of the F-box protein Skp2 in cell proliferation in the developing auditory system in mice. Neuroreport 14, 759–761.

Fero, M.L., Rivkin, M., Tasch, M., Porter, P., Carow, C.E., Firpo, E., Polyak, K., Tsai, L.H., Broudy, V., Perlmutter, R.M., Kaushansky, K., Roberts, J.M., 1996. A syndrome of multiorgan hyperplasia with features of gigantism, tumorigenesis, and female sterility in p27(Kip1)-deficient mice. Cell 85, 733–744.

Izumikawa, M., Minoda, R., Kawamoto, K., Abrashkin, K.A., Swiderski, D.L., Dolan, D.F., Brough, D.E., Raphael, Y., 2005. Auditory hair cell replacement and hearing improvement by Atoh1 gene therapy in deaf mammals. Nat. Med. 11, 271–276.

Kiyokawa, H., Kineman, R.D., Manova-Todorova, K.O., Soares, V.C., Hoffman, E.S., Ono, M., Khanam, D., Hayday, A.C., Frohman, L.A., Koff, A., 1996. Enhanced growth of mice lacking the cyclin-dependent kinase inhibitor function of p27(Kip1). Cell 85, 721–732.

Koff, A., Polyak, K., 1995. p27KIP1, an inhibitor of cyclin-dependent kinases. Prog. Cell Cycle Res. 1, 141–147 [Review] [37 refs].

Lowenheim, H., Furness, D.N., Kil, J., Zinn, C., Gultig, K., Fero, M.L., Frost, D., Gummer, A.W., Roberts, J.M., Rubel, E.W., Hackney, C.M., Zenner, H.P., 1999. Gene disruption of p27(Kip1) allows cell proliferation in the postnatal and adult organ of corti. Proc. Natl. Acad. Sci. USA 96, 4084–4088.

Lumpkin, E.A., Collisson, T., Parab, P., Omer-Abdalla, A., Haeberle, H., Chen, P., Doetzlhofer, A., White, P., Groves, A., Segil, N., Johnson, J.E., 2003. Math1-driven GFP expression in the developing nervous system of transgenic mice. Gene Expr. Patterns 3, 389–395.

Nakayama, K., Ishida, N., Shirane, M., Inomata, A., Inoue, T., Shishido, N., Horii, I., Loh, D.Y., Nakayama, K., 1996. Mice lacking p27(Kip1) display increased body size, multiple organ hyperplasia, retinal dysplasia, and pituitary tumors. Cell 85, 707–720.

Noben-Trauth, K., Zheng, Q.Y., Johnson, K.R., 2003. Association of cadherin 23 with polygenic inheritance and genetic modification of sensorineural hearing loss. Nat. Genet. 35, 21–23.

Raphael, Y., 1993. Reorganization of the chick basilar papilla after acoustic trauma. J. Comp. Neurol. 330, 521–532.

Raphael, Y., Adler, H.J., Wang, Y., Finger, P.A., 1994a. Cell cycle of transdifferentiating supporting cells in the basilar papilla. Hear. Res. 80, 53–63.

Raphael, Y., Athey, B.D., Wang, Y., Lee, M.K., Altschuler, R.A., 1994b. F-actin, tubulin and spectrin in the organ of Corti: comparative distribution in different cell types and mammalian species. Hear. Res. 76, 173–187.

Ruben, R.J., 1967. Development of the inner ear of the mouse: a radio-autographic study of terminal mitoses. Acta Otolaryngol. (Suppl.), 1–44.

Sage, C., Huang, M., Karimi, K., Gutierrez, G., Vollrath, M.A., Zhang, D.S., Garcia-Anoveros, J., Hinds, P.W., Corwin, J.T., Corey, D.P., Chen, Z.Y., 2005. Proliferation of functional hair cells in vivo in the absence of the retinoblastoma protein. Science 307, 1114–1118.

Sasaki, K., Tamura, S., Tachibana, H., Sugita, M., Gao, Y., Furuyama, J., Kakishita, E., Sakai, T., Tamaoki, T., Hashimoto-Tamaoki, T., 2000. Expression and role of p27(kip1) in neuronal differentiation of embryonal carcinoma cells. Brain Res. Mol. Brain Res. 77, 209–221.

Shou, J., Zheng, J.L., Gao, W.Q., 2003. Robust generation of new hair cells in the mature mammalian inner ear by adenoviral expression of Hath1. Mol. Cell. Neurosci. 23, 169–179.

Tarui, T., Takahashi, T., Nowakowski, R.S., Hayes, N.L., Bhide, P.G., Caviness, V.S., 2005. Overexpression of p27Kip1, Probability of Cell Cycle Exit, and Laminar Destination of Neocortical Neurons. Cereb. Cortex. 15, 1343–1355.

Woods, C., Montcouquiol, M., Kelley, M.W., 2004. Math1 regulates development of the sensory epithelium in the mammalian cochlea. Nat. Neurosci. 7, 1310–1318.

ELSEVIER

Bone 39 (2006) 414–419

BONE

www.elsevier.com/locate/bone

Rapid Communication

Resorption of auditory ossicles and hearing loss in mice lacking osteoprotegerin

Sho Kanzaki [a], Masako Ito [c], Yasunari Takada [b], Kaoru Ogawa [a], Koichi Matsuo [b,*]

[a] *Department of Otolaryngology, School of Medicine, Keio University, 35 Shinanomachi, Shinjuku-ku, Tokyo 160-8582, Japan*
[b] *Department of Microbiology and Immunology, School of Medicine, Keio University, 35 Shinanomachi, Shinjuku-ku, Tokyo 160-8582, Japan*
[c] *Department of Radiology, Nagasaki University School of Medicine, 1-7-1 Sakamoto, 852-8501 Nagasaki, Japan*

Received 15 September 2005; revised 16 January 2006; accepted 31 January 2006
Available online 24 March 2006

Abstract

Bones conduct sound in the middle ear. The three ossicles—the malleus, incus, and stapes—form a chain that transmits vibrations from the tympanic membrane to the oval window of the inner ear. Little is known about bone remodeling events in these ossicles and about potential effects of osteoporosis on hearing loss. Osteoclastic bone resorption is enhanced in $Opg^{-/-}$ mice lacking osteoprotegerin, which is a soluble decoy receptor for the osteoclastogenic cytokine RANKL. We asked whether auditory ossicles are resorbed in $Opg^{-/-}$ mice, and whether these mice suffer from impaired auditory function. All three ossicles in $Opg^{-/-}$ mice showed thinning, especially at the malleal manubrium and incus body. Most notably, unlike in the case in wild-type mice, the junction between the stapes and the otic capsule was fixed in $Opg^{-/-}$ mice, and the stapedial footplate was thinner and broader. Radiological analyses revealed that malleal cortical thickness was positively correlated with tibial bone mineral density in $Opg^{-/-}$ and control littermate mice. Furthermore, progressive hearing loss was detected in $Opg^{-/-}$ mice starting at 6 to 15 weeks of age. These data suggest that osteoprotegerin plays a crucial role in hearing by protecting the auditory ossicles and otic capsule from osteoclastic bone resorption.

Keywords: Bone remodeling; Osteoclast; Osteoprotegerin; Hearing loss; Auditory ossicles

Introduction

The three ossicles in the middle ear, the malleus, incus, and stapes, are formed mainly by endochondral ossification of the mesenchyme from the first and second branchial arches [1,2]. The manubrium (handle) of the malleus attaches to the tympanic membrane, while the footplate of the stapes attaches to the oval window of the cochlea. The stapedial foot is mobile and transmits vibrations to the perilymph, the fluid in the inner ear. The inner ear is contained in the otic capsule of the temporal bone, which is the hardest bone in the body.

Bone mineral density (BMD) is determined by the balance between bone resorption by osteoclasts and formation by osteoblasts. Genetic studies of osteopetrotic mice reveal a number of molecules essential for osteoclastogenesis. Osteoclasts differentiate from precursors of the monocyte–macrophage lineage in the presence of the two membrane bound cytokines, macrophage-colony stimulating factor (M-CSF) and RANKL (receptor activator of nuclear factor-κB ligand, also called osteoclast differentiation factor or TRANCE) [3]. The RANKL receptor is a tumor necrosis factor receptor superfamily member known as RANK encoded by the *Tnfrsf11A* gene. RANK signaling in osteoclast precursors activates a series of osteoclastogenic transcription factors including NF-κB, c-Fos/AP-1, and NFATc1 [4–9]. The osteoclastogenic activity of RANKL is masked by the soluble decoy receptor osteoprotegerin (OPG, also called osteoclast inhibitory factor), encoded by *Tnfrsf11B* [10,11]. In bone remodeling, BMD is maintained by a coupling of osteoclastic bone resorption with subsequent osteoblastic formation [12].

In human populations, the incidence of osteoporotic hip fracture increases exponentially with age [13]. Age-related hearing loss, or presbycusis, affects more than one third of individuals above the age of 75 [14]. Although a link between osteoporosis and hearing loss has been suggested [15–17],

* Corresponding author. Fax: +81 3 5360 1508.
E-mail address: matsuo@sc.itc.keio.ac.jp (K. Matsuo).

8756-3282/$ - see front matter © 2006 Elsevier Inc. All rights reserved.
doi:10.1016/j.bone.2006.01.155